Dynamic Piezo-Optic Study of Exciton and Polaron States in AgBr†

G. ASCARELLI
Department of Physics, Purdue University, Lafayette, Indiana 47907
(Received 7 October 1968)

A recently developed piezo-optic technique has been used to study the indirect absorption edge of AgBr. Appreciable structure has been detected. From the variation of the piezo-optic signal as a function of the direction in which the modulating force was applied, it was deduced that the maxima of the valence band are along ⟨111⟩. From the same data, it was deduced that the 1s indirect exciton is split by the valley-orbit interaction into a group of states whose symmetry assignment is $2(\Gamma_4^-+\Gamma_5^-)$ and a group of states whose symmetry assignment is $2\Gamma_3^-$. The energy splitting is 3.8 meV. The exciton series limit is 16.4±0.5 meV above its ground state. From the relative magnitudes of the piezo-optic signal assigned go the 1s exciton states, the magnitudes of the shear deformation potentials of both the phonons and the indirect gap are evaluated as, respectively, −0.58±0.12 and 4.3±0.8 eV. The selection rules for the creation of indirect excitons are discussed. It is observed that the exciton series is repeated whenever the incident photon has an energy that is sufficient to create an exciton whose center of mass has a kinetic energy that is equal to that of the LO phonon at $k=0$. The measured energy of the LO phonon is 17.4±0.5 meV. The exciton series is repeated again whenever the energy of the incident photon is sufficient to create an exciton in which one or both of the constituting polarons may be excited to the edge of their respective polarization wells. The polaron coupling constants of the electron and hole are, respectively, $\alpha_e=1.68\pm0.02$ and $\alpha_h=3.0\pm0.3$. An average of the undressed hole's effective mass that is likely to be close to the value of its transverse mass is $(0.56\pm0.06)m_0$.

I. INTRODUCTION

THE magnetoconductivity and optical absorption[1–6] of AgBr and AgCl indicate that the minimum of the conduction band is at the center of the Brillouin zone and is spherical,[4–6] whereas the valence-band maxima occur at different but equivalent positions in reciprocal space. Theoretical calculations by Bassani *et al.*[7] and Scop[8] indicate that the highest maxima of the valence band are probably at the zone boundary[9] along ⟨111⟩, i.e., at the point L. Subsidiary maxima, with their energy close to that of the highest maxima, are predicted along ⟨100⟩ and ⟨110⟩ and at the point W on the surface of the Brillouin zone. The structure observed in the optical absorption of both AgCl and AgBr[1,3] has been interpreted[7] as due either to excitons made up from electrons excited from inequivalent maxima of the valence band (e.g., at points L and Σ) or due to excitons formed by electrons excited from different bands at equivalent points in reciprocal space when two bands are split by spin-orbit interaction.

Optical absorption in a uniaxially stressed crystal should provide a means for distinguishing between the different assignments of the observed structure. Kanzaki[10] indicated that at helium temperatures irreversible changes in the absorption edge of AgBr take place when stresses of about 6 kg/mm² are applied to the crystal. These changes can be annealed by heating the crystal to 77°K. In Kanzaki's data, there was little indication of splitting of the original structure but mainly smoothing of the sharp absorption edge that appears in the unstressed sample at 4°K.

Important conclusions to be drawn from the above results are that a static stress might not only semipermanently strain the crystal but that the traditional transmission experiments are not able to distinguish the states that are split by the uniaxial stress. The dynamic piezo-optical technique developed by Ascarelli and Barone[11] provides a means of overcoming both difficulties. The increase of sensitivity to structural details that it provides is characteristic of all the recently developed modulation techniques.[12–16] The main advantage of the dynamic piezo-optical measurements over the static ones[17] is that the effective stresses used are in the vicinity of 1 atm, which are insufficient to cause plastic flow.

† Supported in part by the National Science Foundation and Advanced Research Projects Agency.
[1] F. C. Brown, T. Masumi, and J. J. Tippens, J. Phys. Chem. Solids **22**, 101 (1961).
[2] B. L. Joesten and F. C. Brown, Phys. Rev. **148**, 919 (1966).
[3] B. L. Joesten, thesis, University of Illinois, Urbana, 1966 (unpublished).
[4] G. Ascarelli and F. C. Brown, Phys. Rev. Letters **9**, 209 (1962).
[5] H. H. Tippens and F. C. Brown, Phys. Rev. **129**, 254 (1963).
[6] J. W. Hodby, J. A. Borders, F. C. Brown, and S. Foner, Phys. Rev. Letters **19**, 952 (1967).
[7] F. Bassani, R. S. Knox, and W. Beal Fowler, Phys. Rev. **137**, A1217 (1965).
[8] P. M. Scop, Phys. Rev. **139**, A934 (1965).
[9] R. S. Knox (private communication, 1967) informed the author that a revised calculation along the lines of Ref. 7 shows that in AgBr also the maximum of the valence band is expected at the point L.
[10] H. Kanzaki (private communication, 1964).
[11] G. Ascarelli and A. Barone, Nuovo Cimento **37**, 818 (1965); Bull. Am. Phys. Soc. **11**, 644 (1964).
[12] I. Balslev, Phys. Rev. **143**, 636 (1966).
[13] B. O. Seraphin, Phys. Rev. **140**, A1716 (1965).
[14] A. Fovra and P. Handler, Phys. Rev. Letters **14**, 178 (1965).
[15] G. W. Gobeli and E. O. Kane, Phys. Rev. Letters **15**, 142 (1965).
[16] W. E. Engeler, M. Garfinkel, and J. J. Tieman, Phys. Rev. **155**, 693 (1967).
[17] S. E. Schnatterly, Phys. Rev. **140**, A1364 (1965).

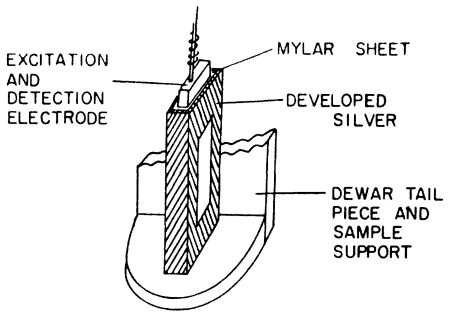

FIG. 1. Diagram of the sample mounted on the sample platform with a schematic illustration of the piston used for the mechanical excitation.

The alternating character of the stress further decreases the importance of plastic deformation.[18]

The aim of this study is to establish the symmetry of the top of the valence band in the silver halides and possibly identify the structure observed in the indirect absorption edge.[1,2] A preliminary report of this work has been published[19] in which it was shown that the valence-band maximum is along ⟨111⟩.

The remaining portion of this paper will describe the experimental technique (Sec. II), and will give a rapid theoretical review of the optical absorption leading to the formation of excitons (Sec. III). The observed exciton and polaron states are discussed in Secs. IV and V. In the conclusion (Sec. VI), the present measurements are related to those of other workers. In Appendix A the symmetries of the different indirect excitons are discussed in detail. The relative magnitudes of the piezooptic signal assigned to some exciton states are calculated in Appendix B. The values of the shear deformation potentials of both the phonons and the valence band at L are obtained. Finally, in Appendix C, the variation of some functions of elastic constants with temperature are obtained from the changes of Young's modulus.

II. EXPERIMENTAL PROCEDURE

A. Piezomodulation Technique

The sample, which is in the shape of a small parallelepiped about $20\times8\times1.5$ mm^3, is made to vibrate in its extensional resonance by using electrostatic excitation (Fig. 1). The technique was initially described in Ref. 11. Silver is developed on most of the sample except on a small window that is used for measurements of the optical properties. The silver electrode on the sample is grounded by resting the sample on the grounded metallic sample holder. On top of the sample there is a small spring-loaded aluminum piston that is electrically insulated from the sample by a 25-μm Mylar sheet. The static stress exerted by the spring-loaded plunger at room temperature is not more than 4×10^4 dyn/cm^2 ($\sim$0.04 atm); because of the appreciable contraction of the sample when the temperature is decreased, this stress should decrease further at low temperature. No signs of plastic flow were detected even after the sample remained mounted on the sample holder for periods of the order of 1 month at a temperature $\sim$77°K. Static strain was monitored with crossed polaroids.

An ac voltage, whose frequency is equal to half the resonance frequency of the sample vibrating in its fundamental extensional mode, is applied to the capacitor formed by the aluminum piston and the top of the sample. The applied voltage, of the order of 500 V rms, produces an electrostatic force between the piston and the sample at a frequency equal to the extensional frequency of the sample.[20] The vibration of the sample is detected by a vibration detector described elsewhere.[20] The main advantage of the electrostatic excitation is that the absence of a transducer avoids the static stresses that are set up by the difference of expansion coefficient of the sample and the transducer or the difference of those of the sample and the material bonding it to the transducer. A disadvantage of the technique is that the ac through the exciting capacitor flows in the electrodes developed on the sample, producing a small heating that is troublesome at helium temperatures in the absence of an exchange gas. This small heating of the sample has been an important source of error in the early measurements; it has been partially overcome by increasing the thickness of the developed silver. A small heating of the sample produces a small change in its elastic constants which in turn produce small changes of its resonant frequency. As a consequence of this frequency shift both the amplitude of vibration and the phase of the mechanical oscillation change with respect to those of the exciting force. These effects are not negligible, since the mechanical Q of the sample is large, between 10^3 and 10^4; frequency changes $\Delta f/f\sim10^{-4}$ are therefore important. The estimated strains were of the order of 10^{-6} but could not be measured as in Ref. 11 in view of the size of the samples. The strain amplitude is limited not only by the inelastic effects evidenced by the change in the sample's resonance frequency ($\sim$0.2%) but also by a decrease in its Q and an increase of the heating effects that increase with increasing applied voltage. The frequency of oscillation varied between about 50 and 100 kHz depending on the exact sample dimensions and its orientation. It is to be stressed that there is no electric field across the sample in this configuration.

The sample support (Fig. 1) is attached to the tailpiece of a conventional optical cryostat. No exchange gas was used between the liquid-helium reservoir and the sample for lack of a transparent material that could

[18] S. N. Zhurkov, B. Ya Levin, and T. P. Sanfirova, Fiz. Tverd. Tela **2**, 1040 (1960) [English transl.: Soviet Phys.—Solid State **2**, 939 (1960)].

[19] G. Ascarelli, Phys. Rev. Letters **20**, 44 (1968). An arithmetic error resulted in absolute energies 1.8 meV too large.

[20] M. Nuovo, Ric. Sci. **31**, (IIA) 212 (1961).

be attached to the thermal shields at liquid helium and could be mounted in such a way as to avoid dichroism due to the stresses produced by the differential thermal expansion between the windows and their support. Furthermore, to avoid breakdown in the gas the pressure has to be below 10^{-3} Torr; under these conditions, the heat-exchange gas is not very effective. The knowledge of the sample temperature is therefore poor: the measured temperature is that of the support (Fig. 1) on which the sample is standing. The *changes* in sample temperature produced either by Joule heating or light absorption may be evaluated by the changes of the resonance frequency of the sample whose amplitude of vibration was continuously monitored. These changes are less than about $\sim 2°K$ for all data reported.

The optical portion of the apparatus consisted of a 0.75-m Spex model 1500 monochromator[21] with a 1200-line/mm grating used in first order; an RCA 7326 photomultiplier with S-20 response; and, as light source, either an Osram HBO/500 high-pressure mercury arc or a quartz-iodine incandescent lamp. No strong mercury lines are present in the region of the spectrum we studied, i.e., between 4410 and 5000 Å.

To filter out some of the noise, the photomultiplier anode current was passed through a high-Q parallel LC tuned circuit ($Q \sim 100$) in series with a 20-kΩ resistor bypassed by a 0.1-μF capacitor. The voltage across the LC circuit tuned to the frequency of the mechanical vibration (equal to twice the applied ac frequency), is the input signal for an emitter follower whose output is synchronously detected.[22] The reference signal for the instrument is obtained by doubling the frequency of the signal exciting the mechanical vibration.

The important parameter to be measured is the change of absorption coefficient of the sample with stress. The voltage produced by the photomultiplier output current on a 20-kΩ resistor bypassed by a 0.1 μF capacitor is the error voltage for the regulated high-voltage power supply that polarizes the photomultiplier. With this stabilization the signal output from the phase-sensitive detector is proportional to the *changes* di, at the frequency of the alternating stress, of the anode current of the photomultiplier whose unmodulated current i_0 is constant; this signal is proportional to the changes dK of the absorption coefficient with stress $d\tau$. The principal source of noise encountered in the measurements was the random fluctuation of the number of photons reaching the photocathode and giving rise to photoelectrons.

The output of the phase-sensitive detector is affected by systematic errors that are due to changes of the index of refraction of the sample with stress. Changes of index of refraction produce changes of the deviation of the light transmitted by the sample and changes of its reflection coefficient. This deviation of the light beam produces changes in the reflection coefficient of both the cryostat windows and the photomultiplier glass envelope as well as changes of the portion of the photocathode that is illuminated at a given instant. These effects give rise to a photosignal that is coherent with the applied stress. They are practically wavelength-independent in the region studied. The effects due to changes in deviation of the transmitted light can be minimized by using a cryostat window having a broad-band antireflection coating on the vacuum side of the cryostat followed by a light pipe whose surface in contact with the window is slightly ground. The light pipe is optically coupled to both the cryostat window and photomultiplier glass envelope with silicone fluid (Dow Corning 200). The spurious signal is decreased in this fashion from a value comparable to that of the desired signal down to a value less than 1% of the maximum of the desired signal. In certain samples in which the faces of the sample are sufficiently parallel and the light has sufficiently normal incidence, the spurious signal is of the order of 0.1% of the desired maximum signal. In all the data reported in this paper, this spurious signal has been subtracted. Its value is assumed to be that of the asymptotic magnitude of the piezo-optic signal in the absence of any optical absorption (e.g., about 150 Å beyond the edge). This shift of zero has been applied to all data. As in Ref. 16, the changes of sample thickness with stress give a negligible contribution to the desired signal.

The output signal from the phase-sensitive detector was displayed on a strip chart recorder; it was also digitized at constant wavelength intervals.[23] These digitized data have been used (after the subtraction of the zero shift produced by the systematic errors discussed above) to make comparisons between the theoretical and observed line shapes. The scatter of the points in such a graph therefore represents a direct measure of the noise output of the system due to all sources.

B. Sample Preparation

Samples were obtained either from an ingot grown in a Br_2 atmosphere by the Bridgman technique from clean AgBr precipitate kindly supplied by Dr. F. Moser and Dr. R. Van Heyningen of the Kodak Research Laboratories, Rochester, N. Y., or from an ingot of zone-refined AgBr kindly provided by Dr. James E. Luvalle of Fairchild Space and Defense Systems, Syosset, N. Y.

Samples from the above sources were cut with a tungsten-carbide saw from an x-ray-oriented crystal. During the cutting, the crystal was lubricated with xylene to decrease the surface damage. After the sample was cut to the proper dimensions (about $20 \times 2 \times 8$ mm^3) it was washed in reagent-grade toluene, triply distilled water, etched in reagent-grade HBr, repeatedly rewashed in distilled water, annealed at 400°C for 24 h, and finally cooled to room temperature in another 24 h. Helium

[21] Spex Industries, Metuchen, N. J.
[22] Electronic Missiles and Communications, Model RJB, Mt. Vernon, N. Y.
[23] A. Onton, thesis, Purdue University, 1967 (unpublished).

TABLE I. Symmetry of the different electronic states and operators that are discussed in the text. The symmetries under the heading "Representations of D_{3d}" correspond to the symmetries of the individual phonon or electron states at L. The symmetry assignments are those of Bassani *et al.*[a] and the notation is that of Koster *et al.*[b] for the states indicated by Γ. The states L_i are in the notation of Bassani *et al.*[a]

		Representations of D_{3d}	Representation of O_h
Valence band	single group	$\Gamma_3^-=L_3^-$	$\Gamma_3^-+\Gamma_4^-+\Gamma_5^-$
maximum at L	double group	$\Gamma_5^-+\Gamma_6^-=L_4^-+L_5^-$	$2\Gamma_8^-$
LA phonon at L		Γ_1^+	$\Gamma_1^++\Gamma_5^+$
LO phonon at L		Γ_2^-	$\Gamma_2^-+\Gamma_3^-+\Gamma_5^-$
TA phonon at L		Γ_3^+	$\Gamma_3^++\Gamma_4^++\Gamma_5^+$
TO phonon at L		Γ_3^-	$\Gamma_3^-+\Gamma_4^-+\Gamma_5^+$
S excitons at L			$2\Gamma_3^-+2\Gamma_4^-+2\Gamma_5^-$
P excitons at L			$2\Gamma_1^++2\Gamma_2^++4\Gamma_3^++6\Gamma_4^++6\Gamma_5^+$
S excitons at Γ (from Γ_8^- and Γ_6^+)			$\Gamma_3^-+\Gamma_4^-+\Gamma_5^-$
P excitons at Γ (from Γ_8^- and Γ_6^+)			$\Gamma_1^++\Gamma_2^++2\Gamma_3^++3\Gamma_4^++3\Gamma_5^+$
Electric dipole			Γ_4^-

[a] Reference 7. [b] Reference 28.

gas passed through a liquid-nitrogen trap to remove traces of oxygen, water and CO_2 flowed in the quartz tube containing the crystal during the annealing. The annealed crystal was polished on a soft cloth wetted with a KCN solution. After the crystal was well polished, no signs of strains could be detected by looking at the crystal through crossed polaroids. The polished crystal was painted with nail polish in the region where transparent windows were desired. After the nail polish had dried, silver was developed on the unprotected parts of the crystal by immersing it in a Kodak D-19 developer solution for a relatively long time (about 10 min for virgin crystals, shorter times in cases when repairs on the electrodes were needed). The nail polish was removed by dissolving it in acetone. The crystals were only exposed to red light ($\lambda>6000$ Å) when their temperature was above about 150°K. The measurements were made on crystals having the long dimension along which the exciting force is applied along ⟨111⟩, ⟨110⟩, or ⟨100⟩.

III. INDIRECT ABSORPTION EDGE

A. Unstressed Crystal

The absorption coefficient corresponding to the case when an exciton is created by a photon whose energy is E, that excites an electron from a state of the valence-band maximum near k in the Brillouin zone (Bz) to a state in the conduction-band minimum near a point k' of the Bz, is[24] (for $E>E_{cr}$)

$$K^j_{k,k'}(E)=\frac{A}{E}[E-E_0{}^j(k,k')\pm\hbar\omega+\delta^j]^{1/2}\times|\Phi_j(0)|^2C^2(n_q+\tfrac{1}{2}\pm\tfrac{1}{2}), \quad (1)$$

[24] R. J. Elliot, in *Polarons and Excitons*, edited by C. G. Kuper and G. D. Whitefield (Oliver and Boyd, London, 1963), p. 269; also, R. S. Knox, *Theory of Exciton* (Academic Press Inc., New York, 1963).

where

$$C(n_q+\tfrac{1}{2}\pm\tfrac{1}{2})^{1/2}=\sum_r\left\{\frac{\langle c,\mathbf{k}',n_q|\,\boldsymbol{\varepsilon}\cdot\mathbf{p}\,|r,\mathbf{k}',n_q\rangle\langle r,k',n_q|\,H_v\,|v,\mathbf{k},n_q\pm1\rangle}{E_v(k)-E_r(k')\pm\hbar\omega(q)}+\frac{\langle c,\mathbf{k}',n_q|\,H_v\,|r,\mathbf{k},n_q\pm1\rangle\langle r,\mathbf{k},n_q\pm1|\,\boldsymbol{\varepsilon}\cdot\mathbf{p}\,|v,\mathbf{k},n_q\pm1\rangle}{E_c(k')-E_r(k)\pm\hbar\omega(q)}\right\}; \quad (2)$$

$K^j{}_{k,k'}=0$ for $E<E_{cr}$. The exciton state is $E_0{}^j$ above the valence band maximum; $E_c{}^{(k')}$ and $E_v{}^{(k)}$ are, respectively, the energies of the conduction-band minimum and the valence-band maximum. In these expressions n_q is the density of phonons of energy $\hbar\omega(q)$ at a temperature T, $\boldsymbol{\varepsilon}$ is the polarization of the light, $\mathbf{p}$ is the momentum operator, H_v is the electron-phonon interaction, $\Phi_j(r)$ is the envelope function describing the jth exciton state, while A involves universal constants, the index of refraction of the material, and the reduced mass of the exciton.

The quantity δ^j, introduced here, is a measure of the broadening of the absorption edge. This broadening is particularly important when $E=E_{cr}{}^j=E_0{}^j\pm\hbar\omega(q)$, the energy necessary to create an exciton, since as will be seen, the piezo-optic measurements detect dK/dE_{cr}, which becomes infinite when $E=E_{cr}{}^j$ and $\delta^j=0$. When the degeneracy of the conduction and valence-band extrema are taken into account, Eq. (1) becomes

$$K^j=\sum_{k,k'}K^j{}_{k,k'}, \quad (3)$$

where the sum is taken over all points of the Bz that belong to the stars of k and k'. In the present case, since the minimum of the conduction band is nondegenerate and at $k'=0$, the sum is over the star of k only.

The exciton wave function can be described by a sum of products of wave functions of the electrons in the conduction band, of the hole in the valence band, and of a modulating function which is a solution of the effective mass equation. The multipeaked valence-band maxima[7–9,19] along ⟨111⟩ are presumably at the edge of the Bz (point L); the corresponding wave functions form the basis for the representation L_3^- of D_{3d} (or for the L_4^- and L_5^- representation of the double group $\bar{D}_{3d}$). Appropriate orthogonal linear combinations of the wave functions[25,26] at L form a bases of representations of O_h (or $\bar{O}_h$). These linear combinations transform[27,28] as Γ_8^- of $\bar{O}_h$. The group-theoretical procedure for obtaining these representations is outlined in Appendix A.

The same procedure may be used to obtain the linear combination of phonons at L which form a basis of the representation of O_h. The results are given in Table I. As in a previous calculation[29] the symmetry of the phonons, of the valence-band states, and of the intermediate state at the center of the Bz are all described in terms of representations of the cubic group $\bar{O}_h$.

The criterion for obtaining the selection rules for band-to-band transitions is for allowed transitions either both the products $\Gamma_v\Gamma_{pn}\Gamma_r$ and $\Gamma_r\Gamma_4^-\Gamma_c$ or both the products $\Gamma_v\Gamma_4^-\Gamma_r$ and $\Gamma_r\Gamma_{pn}\Gamma_c$ must contain Γ_1^+. The representations Γ_v, Γ_r, and Γ_{pn} correspond to the valence-band state, intermediate, and phonon states belonging to $\bar{O}_h$. Transitions involving both LA and TA phonons are allowed while transitions involving optical phonons are forbidden since the latter are odd under inversion.[7,28,29]

The selection rules for the creation of an indirect exciton in a perfect crystal may be obtained by extension of the result for direct excitons[30]: either both $\Gamma_1^+\Gamma_{pn}\Gamma_s$ and $\Gamma_s\Gamma_4^-\Gamma_f$ or both $\Gamma_1^+\Gamma_4^-\Gamma_s$ and $\Gamma_s\Gamma_{pn}\Gamma_f$ must contain Γ_1^+. The quantities Γ_{pn}, Γ_s and Γ_4^-, Γ_f are, respectively, the representations of O_h of the phonons, intermediate exciton states, of the dipole operator and of the final exciton states that contribute to the transition. The representation Γ_1^+ is characteristic of the unperturbed perfect crystal.

Shallow excitons are described by the effective-mass equation in which the perturbation potential is considered to be spherically symmetric varying as $1/r$.[31,32] Some authors[32] have introduced a spherically symmetric correction to this potential to take into account the change of the dielectric constant with r. Within a lattice constant of the center of force, the attractive exciton potential is, however, cubic rather than spherical. As in the case of donors[25–27,33] in Ge or Si the excitons originating from different linear combinations of valence-band states will be split. In the case of S-like excitons

$$\Gamma_{ex}=\Gamma_v\times\Gamma_c\times\Gamma_{env}=2\times\Gamma_8^-\times\Gamma_6^+\times\Gamma_1^+ =2\times(\Gamma_3^-+\Gamma_4^-+\Gamma_5^-).$$

The large spin-orbit interaction of each one of the carriers with the crystal potential is already implicit in the band calculation. Neglecting the spin-spin interaction and the part of the long-range Coulomb interaction[30] that gives rise to longitudinal and transverse excitons, each "orbital" state must be fourfold degenerate on account of the four possible orientations of the electron and hole spin. In this approximation, there are two possible choices for the $1s$ indirect states: either a "singlet" and a "triplet" corresponding respectively to the $2\Gamma_3^-$ and the $2(\Gamma_4^-+\Gamma_5^-)$ representations or two "doublets," each one corresponding to the $(\Gamma_3^-+\Gamma_4^-+\Gamma_5^-)$ representations. The experimental data presented in this paper strongly favors the first alternative. At low temperatures when a stress whose axis is along ⟨111⟩ or ⟨110⟩ is applied to the crystal, the magnitude of the peak assigned to the singlet is the same within experimental error when viewed with light polarized parallel and perpendicular to the stress axis. Such an observation is consistent with what is to be expected from an orbital singlet. The relative amplitudes of the peaks assigned to the triplet and singlet states are expected to be in the ratio 7.8:1 when the external force is applied along ⟨100⟩. This result is obtained under the assumption of the validity of the deformation-potential theory[34] and that intermediate exciton states having $(\Gamma_1^++3\Gamma_5^+)$ symmetry are predominant. Such states could be p-like exciton states formed by a hole at the valence band maximum at L and an electron at the conduction band extremum at Γ having Γ_8^+ symmetry.[7] The experimental value of this ratio is 8 ± 2. The question is treated in further detail in Appendix B. This splitting of the $1s$ exciton states obtained from different equivalent band extrema is called "valley-orbit splitting" in the semiconductor literature.[7,25,26,33,35] It has not been observed in excitons in Ge and Si presumably on account of the small binding energies involved.

A further splitting of the fourfold-degenerate $2\Gamma_3^-$ state cannot be excluded although it is not observed. A possibility might be, e.g., that the two pairs of Γ_3^- states correspond to parallel and antiparallel orientations of the electron and hole spins. In the present case the exciton radius is much larger than an atomic Bohr radius and the splitting should therefore be smaller than in the case of positronium. The splitting of the triplet into four threefold-degenerate states whose symmetries

[25] W. Kohn and J. M. Luttinger, Phys. Rev. **98**, 915 (1955).
[26] J. Appel, Phys. Rev. **133**, A280 (1964).
[27] A. K. Ramdas, P. M. Lee, and P. Fisher, Phys. Letters **7**, 99 (1963).
[28] G. F. Koster, J. O. Dimmock, R. G. Wheeler, and H. Statz, *Properties of the Thirty Two Point Groups* (M.I.T. Press, Cambridge, Mass., 1963).
[29] M. Lax and J. J. Hopfield, Phys. Rev. **124**, 115 (1961).
[30] J. J. Hopfield, Phys. Chem. Solids **15**, 97 (1960).
[31] G. Dresselhauss, Phys. Chem. Solids **1**, 14 (1956).
[32] V. M. Buimistrov, Fiz. Tverd. Tela **5**, 3264 (1963) [English transl.: Soviet Phys.—Solid State **5**, 2387 (1964)].
[33] D. K. Wilson, Phys. Rev. **134**, A265 (1964).
[34] C. Herring and E. Vogt, Phys. Rev. **101**, 144 (1956).
[35] T. P. McLean and R. Loudon, Phys. Chem. Solids **13**, 1 (1960).

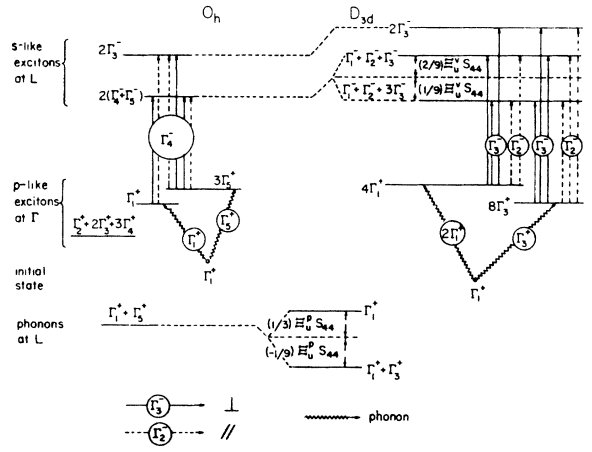

FIG. 2. 1s exciton and LA phonon states obtained taking into account the multipeaked character of the valence band. The effect of a uniaxial unit stress along ⟨111⟩ that decreases the crystal symmetry from O_h to D_{3d} is shown. In this figure it is assumed that the 1s exciton triplet in the strained crystal is split into a state having $(\Gamma_1^-+\Gamma_2^-+\Gamma_3^-)$ symmetry and a state having $(3\Gamma_3^-+\Gamma_1^-+\Gamma_2^-)$ symmetry. These symmetry assignments are justified by the success in the explanation of the magnitude of the exciton peaks (Appendix B). The p-like exciton intermediate state obtained from the Γ_8^- valence band and the Γ_6^+ conduction band is also shown. No attempt has been made to consider splittings, if any, that may exist among states of different symmetry. The splittings of the p exciton states shown in the figure are only to simplify the drawing. In the case of the stressed crystal only the intermediate p-like exciton states that contribute to the transition are shown.

are Γ_4^-, Γ_4^-, Γ_5^-, and Γ_5^-, may arise from both spin-spin and long-range Coulomb interactions.[30]

In Eqs. (1)–(3) the contributions of only one type of process to the absorption edge have been considered. There will be energies of the photon for which more than one final state (j) is possible, e.g., excitons might be formed in any one of a series of excited states.

Expression (3) is therefore modified into

$$K=\sum_j \sum_{k,k'} K^j{}_{k,k'}. \tag{4}$$

An important case when the sum over j will modify the absorption spectrum is when the photon energy is sufficient to create excitons close to the series limit. Exciton states whose principal quantum number is $n\geq n_{\min}$ shall be considered as being merged with the exciton series limit. The choice of $n_{\min}$ is determined by the resolution of the instrument. A value in the vicinity of 3 is adequate for the present case.

The exciton states that are more easily reached in optical absorption are s states for which $|\Phi_j(0)|^2$ is largest.[24] Although corrections to the effective-mass approximation are important for the $n=1$ exciton states, higher states are well described by a hydrogenlike series for which $|\Phi_{n,0}(0)|^2$ decreases as n^{-3}.

Only a limited number of states have been detected; states for which $n>3$ appear to be merged into a continuum. A photon whose energy is E can create excitons in a state whose quantum number $n\leq n_{\max}$ is determined by

$$E=E_g\pm\hbar\omega-E_x/n_{\max}{}^2. \tag{5}$$

E_x is the exciton binding energy. The contribution of s-like exciton states to the absorption coefficient associated with the exciton series limit is obtained by transforming Eq. (4) into an integral:

$$K_s'=K_s\rho_s$$
$$=K_s\int_{n\min}^{n_{\max}} n^{-3}\left(E-E_g\mp\hbar\omega+\frac{E_x}{n^2}+\delta\right)^{1/2}dn, \tag{6}$$

from which

$$\rho_s=\frac{E_x{}^{1/2}}{3n_{\min}{}^3}\left[1-\left(\frac{E_g\pm\hbar\omega-E-\delta}{E_x}\right)n_{\min}{}^2\right]^{1/2}. \tag{7}$$

The contribution to the absorption coefficient from the remaining states whose angular momentum $l\neq 0$ and even is small since $|\Phi_{n,j}|^2$ is very small in the neighborhood of the hole. For each value of $n\gg 1$ there are $\frac{1}{2}n^2$ of these states.

Under the assumption that $|\Phi_{n,l}(0)|^2$ is the same for all l the absorption coefficient is

$$K_l'=K_l\rho_l$$
$$=K_l\int_{n\min}^{n_{\max}}\frac{n^2}{2n^3}\left(E-E_g\mp\hbar\omega+\frac{E_x}{n^2}+\delta\right)^{1/2}dn \tag{6'}$$

and

$$\rho_l=K_lE_x{}^{1/2}\left\{\left[1-\left(\frac{E_g\mp\hbar\omega-\delta-E}{E_x}\right)n_{\min}{}^2\right]^{1/2}n_{\min}{}^{-1}-\left(\frac{E_g\mp\hbar\omega-\delta-E}{E_x}\right)^{1/2}\times\left[\tfrac{1}{2}\pi-\sin^{-1}\left(\frac{E_g\mp\hbar\omega-\delta-E}{E_x}n_{\min}{}^2\right)^{1/2}\right]\right\}.$$

The absorption coefficient due to all these highly excited states will be

$$K=K_s\rho_s(E)+K_l\rho_l(E). \tag{8}$$

At energies sufficiently large for the light to produce free-electron hole pairs another term in the expression giving the absorption coefficient becomes important.[24] This term is proportional to $(E-E_g\pm\hbar\omega)^2$. Other sources of changes in the optical-absorption coefficient are discussed in Ref. 24, e.g., absorption into single exciton states becomes again proportional to $(E-E_g\pm\hbar\omega)^{1/2}$ for photon energies appreciably above the exciton continuum.

B. Effect of Stress on the Absorption Coefficient

A small stress $d\tau$ will split the energy of the equivalent maxima of the valence band[34] and consequently the

degenerate exciton states.[33] In the case of a single type of process j giving rise to the optical absorption the changes dK^j of the absorption coefficient are

$$\frac{dK^j}{d\tau}=\sum_k \frac{dK_k{}^j}{d[E_{cr}(k)-\delta^j(k)]}\frac{d[E_{cr}(k)-\delta^j(k)]}{d\tau}. \quad (9)$$

Instead of summing over the equivalent points of the Bz forming the star of k the sum may be taken over the different linear combinations of exciton states that transform according to a given irreducible representation. The quantity $dK_k{}^j/d[E_{cr}(k)-\delta^j(k)]$ is the same for all exciton states while the term

$$\frac{d[E_{cr}(k)-\delta^j(k)]}{d\tau}d\tau$$

reflects the change with stress of both the energy and the linewidth of the individual exciton states. Transforming Eq. (9) into a sum over the different representations Γ_i of the excitons in the stressed crystal one obtains

$$\frac{dK^j}{d\tau}=\frac{dK^j}{d(E_{cr}{}^j-\delta^j)}\sum_{\Gamma_i}\frac{d[E_{cr}{}^j(\Gamma_i)-\delta^j(\Gamma_i)]}{d\tau}. \quad (10)$$

For a given stress the sum may be either positive or negative, giving rise to increases or decreases of optical absorption.

It is not possible from symmetry arguments alone to provide criteria for associating the states that remain quasidegenerate when the exciton states are split by stress. When a force is applied along ⟨100⟩ all the ⟨111⟩ maxima of the valence band are equally affected.[34] No relative changes among the energies or "linewidths" corresponding to different excitons are expected in this case. Accordingly, "peaks" traced to changes of the exciton creation energy or linewidth should have the same relative magnitudes when viewed with light polarized parallel and perpendicular to the applied force. In particular, the orbital triplet group of nearly degenerate states whose symmetry is $2(\Gamma_4^-+\Gamma_5^-)$ will not be split when the crystal symmetry is reduced from $\bar{O}_h$ to $\bar{D}_{4h}$.

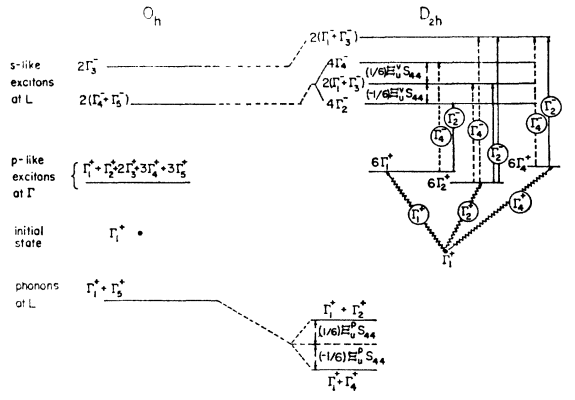

FIG. 3. 1s exciton and LA phonon states obtained taking into account the multipeaked character of the valence-band states. The effect of a ⟨110⟩ stress is shown. In the stressed crystal only the symmetry of the intermediate p-like exciton states that contribute to the transition are shown. The splittings of the intermediate state that are shown are only for the convenience of the drawing.

When a force is applied along the ⟨111⟩ or ⟨110⟩, the crystal symmetry is reduced, respectively, to $\bar{D}_{3d}$ and $\bar{D}_{2h}$ and the orbital triplet exciton states will be split in two or three different orbital states. The corresponding changes in the energy of creation of the split excitons with respect to the center of gravity of the exciton energies may be calculated using the theory for the donor ground state in Ge.[33] The energy shifts (not to scale) produced by the stress are shown in Figs. 2 and 3. The resulting peaks should be appreciably different when viewed with light polarized parallel and perpendicular to the applied force. Furthermore, the spectrum obtained with a crystal subject to a ⟨110⟩ force and observed with light polarized perpendicularly to the stress axis should depend on the direction of propagation of the light since two axes perpendicular to each other and to the direction of the applied force are nonequivalent.

Two types of terms contribute to $dK^j/d\tau$: changes in the energy of creation and linewidth of the exciton states, and changes in the matrix elements used in the description of the optical absorption.

$$\frac{dK^j}{d\tau}=-\tfrac{1}{2}AC^2|\Phi_j(0)|^2(n_q+\tfrac{1}{2}\pm\tfrac{1}{2})(E-E_{cr}{}^j+\delta^j)^{-1/2}E^{-1}\left\{\sum_i\frac{d}{d\tau}(E_{cr}{}^j(\Gamma_i)-\delta^j(\Gamma_i))+4\frac{E-E_{cr}{}^j+\delta^j}{C}\frac{dC}{d\tau}\right\}, \quad (11)$$

where

$$\frac{dC}{d\tau}=\sum_{r,t,m}\frac{dC}{d[E_v(\Gamma_t)-E(\Gamma_r)\pm\hbar\omega(\Gamma_m)]}\frac{d}{d\tau}[E_v(\Gamma_t)-E(\Gamma_r)\pm\hbar\omega(\Gamma_m)]$$

$$+\sum_{r,m}\frac{dC}{d[E_c-E(\Gamma_r)\pm\hbar\omega]}\frac{d}{d\tau}[E_c-E(\Gamma_r)\pm\hbar\omega(\Gamma_m)]-\sum_r\left\{\frac{\langle r|H_v|v\rangle}{E_v-E_r\pm\hbar\omega}\frac{d}{d\tau}[\langle c|\boldsymbol{\varepsilon}\cdot\mathbf{p}|r\rangle]\right.$$

$$\left.+\frac{\langle c|\boldsymbol{\varepsilon}\cdot\mathbf{p}|r\rangle}{E_v-E_r\pm\hbar\omega}\frac{d}{d\tau}[\langle r|H_v|v\rangle]+\frac{\langle c|H_v|r\rangle}{E_c-E_r\pm\hbar\omega}\frac{d}{d\tau}[\langle r|\boldsymbol{\varepsilon}\cdot\mathbf{p}|v\rangle]+\frac{\langle r|\boldsymbol{\varepsilon}\cdot\mathbf{p}|v\rangle}{E_c-E_r\pm\hbar\omega}\frac{d}{d\tau}[\langle c|H_v|r\rangle]\right\}. \quad (12)$$

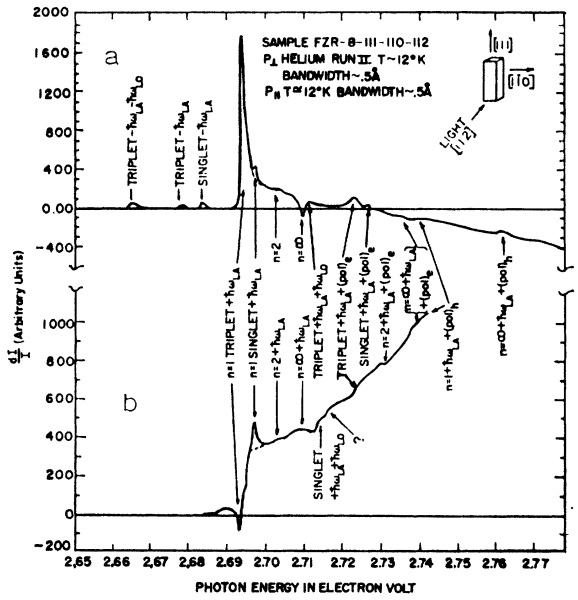

FIG. 4. Piezo-optic signal obtained when the exciting force is along [111]. In the upper figure (a) the polarization of the light is along [1$\bar{1}$0] while in the lower figure (b) it is along [111]. 1500 arbitrary units correspond approximately to $dI/I=10^{-3}$. The broken lines indicate the baseline for the calculation of Appendix B.

As pointed out earlier, if $\delta=0$ whenever $E=E_{cr}$ there would be an infinite peak in the piezo-optic signal decaying to zero as $(E-E_{cr})^{-1/2}$. It should be noted that its contribution to $dK/d(E_{cr}-\delta)$ is negative.

Some information on the intermediate state contributing to the optical transition may be obtained from the piezo-optic signal. If the most important intermediate states having Γ_7 symmetry [in Eq. (12)] are those at a point L at the edge of the Bz ,then they are not split by a force directed along ⟨100⟩, and the linear terms in $(E-E_{cr}{}^j)$ of

$$E(E-E_{cr}{}^j)^{1/2}(dK^j/d\tau)$$

due to changes of either the matrix elements or the energy of the intermediate state should not depend on the direction of polarization of the light. If, instead, important states contributing to the optical transition are degenerate states at the top of the valence band at Γ that, e.g., have Γ_8^- symmetry,[7] a force applied in any crystalline direction will remove the fourfold degeneracy[36] and the effect of changes in $dC/d\tau$ will be different with light polarized parallel and perpendicular to the applied force. The signal originating from $dC/d\tau\neq 0$ is called "background" in Sec. III.

The sign and energy dependence of $\sum_j dK^j/d(E_{cr}-\delta)$ corresponding to the exciton series limit is different from that of an isolated exciton state. Furthermore, since the higher exciton states are well described by the effective mass approximation,[24,33] $d(E_{cr}-\delta)=d(E_g\pm\hbar\omega-\delta)$.

Differentiating Eq. (7) with respect to $(E_g\pm\hbar\omega-\delta)$,

$$\frac{dK_s'}{d(E_g\pm\hbar\omega-\delta)}=K_s\frac{E_x^{1/2}}{2n_{\min}{}^3}\left(1-\frac{E_g\pm\hbar\omega-\delta-E}{E_x}n_{\min}{}^2\right)^{1/2}. \quad (13)$$

It is expected that this expression shall give the largest contribution to the exciton series limit. Therefore,

$$\left[\left(\frac{aK}{dE_{cr}}\right)_{\substack{\text{series}\\ \text{limit}}}\right]^2\propto 1-\frac{E_g\pm\hbar\omega-\delta-E}{E_x}n_{\min}{}^2. \quad (14)$$

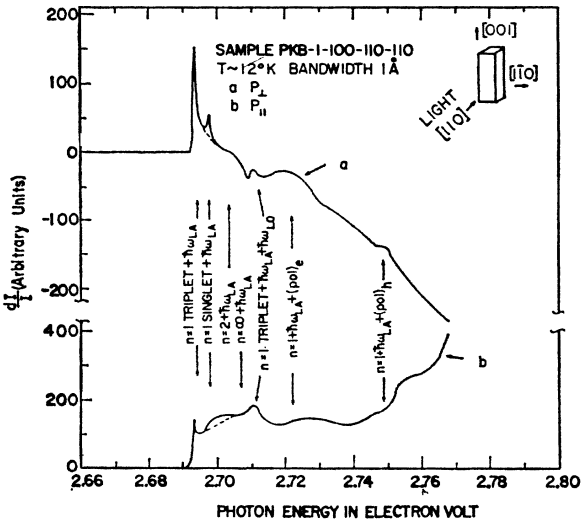

FIG. 5. Piezo-optic signal obtained when the exciting force is along [001]. In the upper curve (a) the polarization of the light is along [110] while in the lower curve (b) it is along [001]. Approximately 1000 arbitrary units correspond to $dI/I=10^{-3}$. The broken lines indicate the baseline for the calculation of Appendix B.

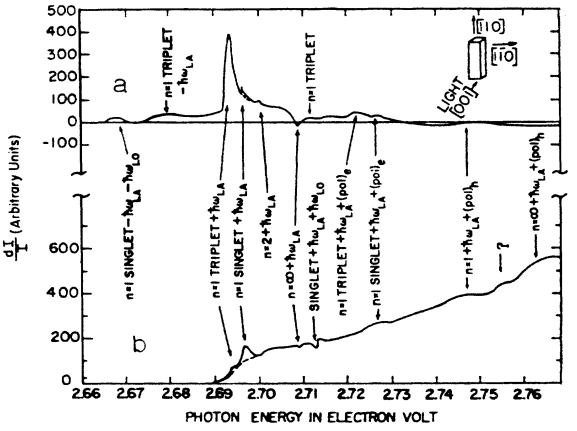

FIG. 6. Piezo-optic signal obtained when the exciting force is along [110]. Upper curve (a) signal observed with light polarized along [1$\bar{1}$0]. Lower curve (b) observed with light polarized along [110]. 1500 arbitrary units correspond approximately to $dI/I=10^{-3}$. The broken lines indicate the baseline for the calculation of Appendix B.

[36] G. E. Pikus and G. L. Bir, Fiz. Tverd. Tela **1**, 1642 (1959) [English transl.: Soviet Phys.—Solid State **1**, 1502 (1960)].

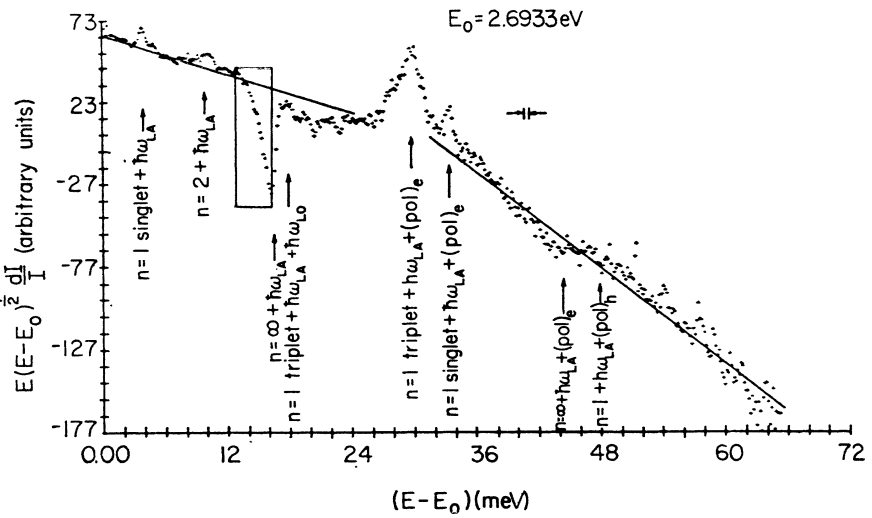

FIG. 7. Data of Fig. 4(a) multiplied by $E(E-E_0)^{1/2}$, where $E_0=2.6933$ eV corresponds to the largest peak observed in Fig. 4(a). The data are obtained from the digitized output of the phase-sensitive detector. The framed portion is plotted in Fig. 8.

The terms originating from $dK_l/d(E_{cr}-\delta)$ will contribute terms of the type $(E_g\pm\hbar\omega-E)^m$ $(m>0)$ and a term proportional to $(E_g\pm\hbar\omega-E-\delta)^{-1/2}$.

Although the latter diverges when $(E_g\pm\hbar\omega-E)\to 0$, its importance will be decreased by the finite value of δ and by the fact that $K_l\ll K_s$ (since $|\Phi_{n,l}(0)|^2\sim 0$).

It is to be noticed that the exciton series limit will give rise to a peak that has a sign that is opposite to that of the leading term in Eq. (11) if $dE_{cr}/d\tau$ has the same sign in both cases.[37]

IV. EXPERIMENTAL RESULTS: EXCITON STATES

In Figs. 4–6 the experimental results for a sinusoidal force applied along ⟨111⟩, ⟨100⟩, and ⟨110⟩ directions are shown; the measured temperature is ~12°K.

In the case of an external force directed along [111] and light polarized along [110] [Fig. 4(a)], a very prominent peak is observed at 2.6933 eV. This energy is assigned to the creation of an indirect exciton in a $1s$ state belonging to $2(\Gamma_4^-+\Gamma_5^-)$ of O_h. It corresponds to the orbital $1s$ triplet state considered previously. Following previous authors[1,2,7] it is assumed that a LA phonon is emitted in the transition. Figure 4(b) corresponds to the same sample as in Fig. 4(a), in which the optical signal is observed with light polarized along [111]; the peak at 2.6933 eV has now a sign that is opposite to that of Fig. 4(a). The state giving rise to this peak is therefore split by a force applied along ⟨111⟩. The different states contributing to the sum of Eq. (10) give in this case such different contributions that even the sign of the sum corresponding to the different polarizations is changed.

[37] If the change in the value of $|\Phi(0)|^2\propto 1/n^3$ that would be expected from a purely hydrogenic model had not been taken into account, then the resulting sign of the piezo-optical signal would not have been opposite to that due to the singlet state.

When the force is applied instead along [100] and the light used for the measurement is polarized parallel or perpendicular to [100] (Fig. 5) the observed peak at 2.693 eV has the same sign and magnitude in both cases indicating that a force along ⟨100⟩ does not split the exciton peaks. The valence-band maxima are therefore along ⟨111⟩, as described previously.[19] A further confirmation of this symmetry assignment is obtained when the applied force is along [110] and the direction of polarization of the light is either along [1$\bar{1}$0] or [110] (Fig. 6). The signal corresponding to the 2.693-eV peak has a drastically different appearance when viewed with light polarized in the two directions.

The peak 3.8 meV above that assigned to the exciton triplet is assigned to the singlet exciton. The same LA phonon is emitted in both cases. This peak has always the same sign and nearly the same magnitude (Figs. 4–6) with respect to the background when observed with light polarized either parallel or perpendicular to the applied force; it is therefore probably not split by a force applied along any of the three principal crystal directions, indicating that it should indeed be assigned to the singlet exciton state.

Small peaks assigned to the creation of excitons with absorption of a LA phonon are observed 15 meV below each of the peaks assigned to the creation of the singlet and triplet exciton with the emission of a phonon [Figs. 4(a) and 6(a)]. The energy of the LA phonon so determined (7.5 meV) is in good agreement with that of other authors.[1–3] The relative magnitudes of the peaks assigned to the creation of excitons with the absorption and emission of phonons will be discussed in more detail later (Appendix B).

Other evidence supporting the assignment of the 2.6933-eV peak to an exciton is given in Fig. 7. The piezo-optic signal multiplied by $E(E-E_0)^{1/2}$ is plotted as a function of $E-E_0$, where E_0 is the energy necessary to create a triplet exciton with the emission of a phonon.

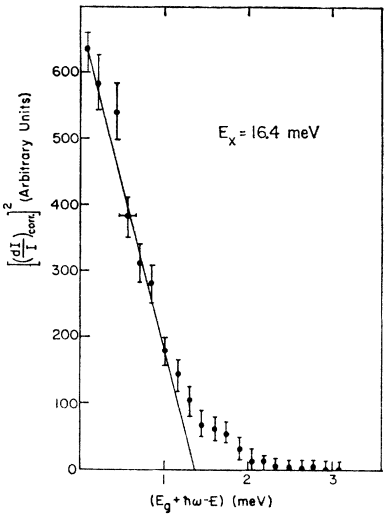

FIG. 8. Data of Fig. 7 in the vicinity of $E-E_0=16.4$ meV. For details of the meaning of the ordinate axis see text.

Equation (11) indicates that when $dC/d\tau=0$ such a plot should be a straight line parallel to the energy axis; when $dC/d\tau\neq 0$ the plot should provide a straight line inclined with respect to the energy axis. The data presented in Fig. 7 indicate such a dependence. The fact that the slope of such a line depends on the direction of polarization of the light even when the applied force is along [100] indicates that intermediate states at Γ split by stress are the most important for this optical transition. A likely intermediate state is formed by the creation of indirect excitons involving higher conduction band states at Γ having Γ_8^+ symmetry.[7,8]

Another peak is prominent in Figs. 4–7 at 2.7096 eV and has a sign opposite to that assigned to the $1s$ singlet exciton. It is assigned to the exciton series limit. When this peak is plotted as a function of $E-E_\infty$, where $E_\infty=E_g+\hbar\omega$ (Fig. 8), it is observed that it has an energy dependence consistent with Eq. (14). The data for this plot are obtained from the framed points in Fig. 7 by subtracting the portion of the straight line through its base, as indicated in Fig. 7. The adjustable parameters used are the position of the peak (varied by ± 0.2 meV) and the possible slopes of the straight line of Fig. 7. Such extremely small adjustments have some effect only on the points near the peak and near the tail of the "line." In Figs. 4–7 a small peak is observed at 2.7055 eV; it is assigned to an $n=2$ exciton state, possibly a $2s$ triplet. This state is thus 10.4 meV above the $1s$ triplet.

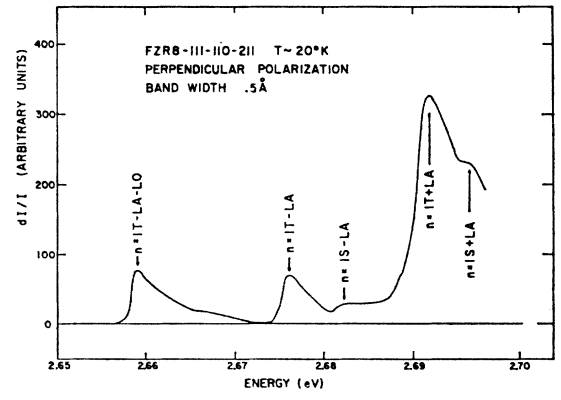

FIG. 9. Piezo-optic signal obtained on a sample stressed along [111] and observed with light polarized along [110]. The measured temperature is 20°K.

The relative magnitudes of the triplet and singlet exciton lines have been evaluated by calculating the sums appearing in Eq. (10). Three adjustable parameters were used and the linewidths δ^j were assumed to be independent of stress. Two of the parameters are the ratio of $3\Xi_u{}^v s_{44}$ and $3\Xi_u{}^p s_{44}$ to the changes of the indirect energy gap when the crystal is subject to a unitary hydrostatic stress. The quantities $\Xi_u{}^p$ and $\Xi_u{}^v$ are, respectively, the shear deformation potentials of the LA phonons[38] and the valence-band maxima at L; s_{44} is the shear complicance constant. The third parameter is

$$\varphi=[|\Phi_t(0)|^2(\delta^s)^{1/2}]/[|\Phi_s(0)|^2(\delta^t)^{1/2}].$$

The symbols t and s stand for triplet and singlet. Details of the calculation are given in Appendix B. Good agreement is obtained between the measured and calculated relative magnitudes of the peaks assigned to the creation of a singlet and triplet exciton. This agreement supports the symmetry assignments of the exciton states (Figs. 2 and 3) and indicates that the p-like exciton formed by a hole at the top of the valence band at Γ and an electron at the bottom of the conduction band at Γ is indeed the most important intermediate state contributing to the transition. Other conclusions of the calculation are that

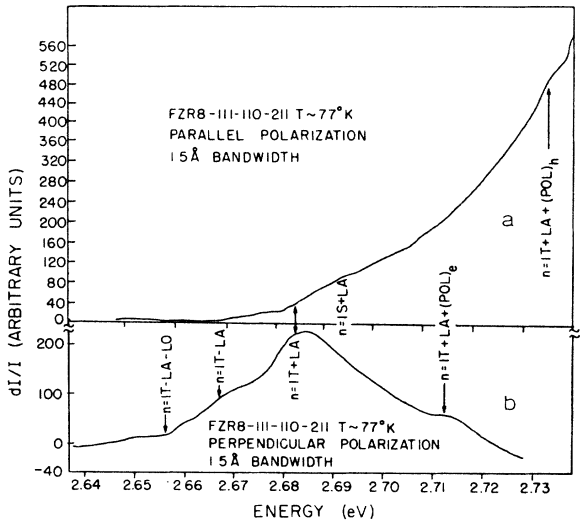

FIG. 10. Piezo-optic data obtained from a sample at ~77°K. The stress axis is [111]. Upper trace (a) light polarized along [111], lower trace (b) light polarized along [110].

[38] G. S. Hobson and E. G. S. Paige, Proc. Phys. Soc. (London) 88, 437 (1966).

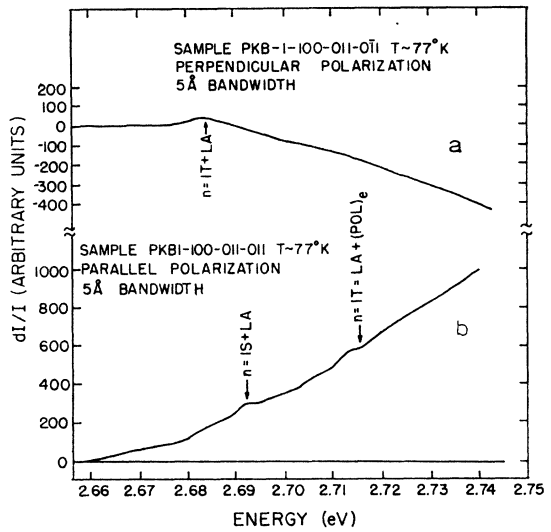

FIG. 11. Piezo-optic signal obtained from a sample at ~77°K. The stress axis is [100]. Upper curve (a) light polarized along [011], lower curve (b) light polarized along [100].

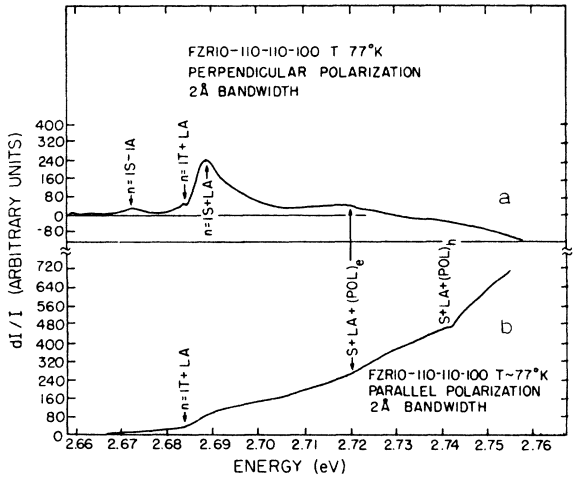

FIG. 12. Piezo-optic signal obtained from a sample at ~77°K. The stress axis is [110]. Upper trace (a) light polarized along [1$\bar{1}$0]. Lower trace (b) light polarized along [110].

the shear deformation potential of the LA phonon is small compared with that of the valence band ($\sim\frac{1}{8}$). The changes of energy of the LA phonons and of the energy gap of a hydrostatically deformed crystal are instead comparable. These large phonon deformation potentials are not astonishing in view of the large changes of the elastic constants of ionic crystals with both stress[39,40] and temperature (Appendix C).

Upon increasing the sample temperature, two qualitatively different effects become noticeable (Fig. 9): a broadening of the exciton peaks and an increase of the magnitude of the peaks assigned to the creation of an exciton, with the absorption of a phonon compared to the case when a phonon is emitted. The enhancement of the probability of creation of an exciton with the absorption of a phonon is to be expected from Eq. (1) due to an increase in $n(q)=(1-\exp(\hbar\omega/kT))^{-1}$ with temperature. The broadening of the exciton peaks is assigned to changes of the linewidth δ with temperature.

The data shown in Figs. 10 and 11 corresponds to the case when the external force is applied along either [100] or [111] and the temperature is about 77°K. It may be explained on the basis of a broadening of all peaks and an enhancement of the peaks assigned to the case when an exciton is created with the absorption of a phonon. This simple explanation is unsatisfactory in the case when the applied force is along [110] (Fig. 12). At 12°K when the exciting mechanical force is along [110] and the direction of polarization is along [1$\bar{1}$0] (Fig. 6), the peak assigned to the creation of a 1s singlet orbital exciton is appreciably smaller than the peak assigned to the triplet. At 77°K instead, the peak assigned to the singlet is larger than that assigned to the triplet. This observation is interpreted as an indication that the linewidth of the excitons depends appreciably on the symmetry and magnitude of the stress tensor. The quantity $d\delta/d\tau$ contributes therefore to the piezo-optic signal.

Another effect whose contribution is difficult to gauge is the creation of indirect excitons in conjunction with the absorption or emission of a TA phonon. Such processes are allowed on the basis of the selection rules.

At 12°K some indication of the existence of a transition in which a TA phonon is involved appears in the data obtained when the applied force and polarization of the light are both along [111] [Fig. 4(b)]. There appears to be some structure both between the peaks assigned to the creation of a singlet and triplet 1s exciton with the emission of a LA phonon and on the low-energy side of the peak assigned to the creation of a 1s triplet exciton with the emission of a LA phonon. In the calculation of the relative magnitudes of the singlet and triplet peaks these signals were assigned to a not-better-identified "background." The same is valid for the region underlying the triplet peak observed with stress and polarization along [110] [Fig. 6(b)] and on the low-energy side of the triplet peak [Figs. 6(a) and 6(b)]. If such a structure is assigned to the creation of excitons with the help of TA phonons, it would indicate that the latter have an energy of about 5 meV. Such an energy

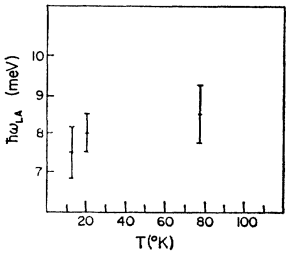

FIG. 13. Apparent variation of the energy of the LA phonons with temperature. The phonon energy is obtained from half the difference of the energies of the peaks assigned to the creation of a triplet (or singlet) exciton with the absorption and the emission of a LA phonon.

[39] K. M. Koliwad, P. B. Ghate, and A. L. Ruoff, Phys. Status Solidi **21**, 507 (1967).

[40] J. H, Parker, E. F. Kelly, V. I. Bolef, Appl. Phys. Letters **5**, 7 (1964); **5**, 64 (1964).

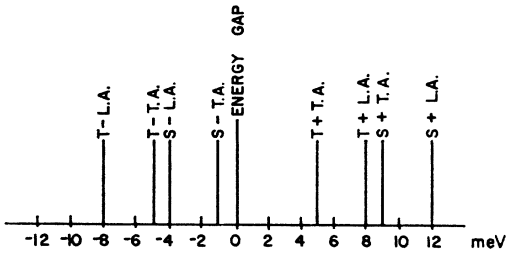

FIG. 14. Sketch of the relative positions of the energy gap and of the peaks assigned to the creation of excitons with the absorption or emission of a LA or TA phonon. The energies of the LA and TA phonons are assumed to be, respectively, 8 and 5 meV.

would be close to what one would expect from the ratio of the velocities of LA and TA low-frequency phonons[41] propagating along ⟨111⟩ (~2.1:1).

Another evidence for the existence of a transition involving a TA phonon arises from the anomalous *increase* of the LA phonon energy with temperature (Fig. 13); such a dependence is opposite to what is expected from the temperature dependence of the elastic constants (Appendix C). A possible explanation may be obtained when one considers the temperature dependence of the probability of creation of excitons in which LA or TA phonons are involved. The peak assigned to the creation of a singlet exciton with the absorption of a LA phonon should be at an energy about 1 meV higher than that corresponding to the creation of a triplet exciton with the absorption of a TA phonon (Fig. 14). These peaks are not experimentally distinguishable. Upon increasing the sample temperature the ratio of the probability of creation of an exciton with the absorption of a TA and LA phonon increases as

$$[1-\exp(\hbar\omega_{TA}/kT)]/[1-\exp(\hbar\omega_{LA}/kT)].$$

It is possible that upon increasing the temperature to ~77°K the peak originating from the TA phonon becomes progressively dominant. This produces an apparent shift towards lower energies of the peak assigned to the creation of a singlet exciton with the absorption of a LA phonon. Since the energy of the phonon is determined by the energy difference of the peaks assigned to the creation of an exciton with the absorption and emission of a phonon this shift produces an apparent increase of the phonon energy with temperature. A similar process may be expected by the combination of the peaks assigned to the creation of a triplet exciton with the emission of a LA phonon and that of the peak to be assigned to the creation of a singlet exciton with the emission of a TA phonon. The apparent energy of the peak assigned to the LA phonon will increase with temperature. The rapid broadening of the exciton peaks with temperature and the increased importance of the contribution to the piezo-optic signal of the changes of linewidth with stress make it difficult to accurately locate the positions or calculate the relative magnitudes of the peaks due to processes in which a LA phonon is involved. This further complicates the analysis of the data.

[41] K. Brugger, J. Appl. Phys. **36**, 759 (1965).

V. TRANSITION INTO POLARON STATES

Polaron effects may modify the absorption edge of an ionic crystal.[42] The structure observed at energies higher than what is assigned to the exciton series limit is interpreted as arising from this source.

Such states are seen in Figs. 4–6 at energies ~17.4 meV above either the line assigned to the triplet or the singlet exciton—the most prominent of the two lines is that corresponding to the formation of the triplet exciton, when the regular triplet exciton line is more prominent. The triplet exciton line in which the exciton has a kinetic energy $\hbar\omega_0$ is partially masked by the structure assigned to the exciton series limit.

At energies below the band gap, structure observed at 2.666 eV is assigned to the case when the LO phonon energy is provided by the lattice. Traces of such a signal are seen in Fig. 4; as expected they are enhanced at higher temperatures (Fig. 9). At still higher temperatures (77°K), with the general broadening of the lines, traces of such states are indicated by changes of slope.

When a polaron is created with kinetic energy larger or equal to that of a LO phonon a degenerate state exists in which the carrier has zero kinetic energy and an LO optical phonon is emitted. There is a singularity in the polaron density of states when this new process becomes possible.[43,44] Excitons may be created when the LO phonon is absorbed rather than emitted.[42] On account of parity, however, this indirect transition is only possible if the wave vector of the optical phonon is different from zero; the transition is allowed in an order of perturbation theory beyond that of the usual indirect absorption.

The LO phonon energy (17.4 meV) obtained in this fashion is in excellent agreement with the direct measurements of Brandt and Brown[45] (17.6 meV), with the values obtained from mobility measurements,[46] or by the application of the Lyndane-Sachs-Teller relation[47] to the measured TO phonons.

In InSb, pinning of the conduction-band Landau levels at the energy of the LO and TO phonon energy has been observed[48,49] and interpreted as evidence for

[42] R. Heck and T. O. Woodruff, Bull. Am. Phys. Soc. **13**, 26 (1968); and private communication.
[43] G. D. Whitfield and R. Puff, Phys. Rev. **139**, A338 (1965).
[44] B. Velicky, in *Optical Properties of Solids*, edited by J. Tauc (Academic Press Inc., New York, 1966), p. 379.
[45] R. C. Brandt and F. C. Brown, Bull. Am. Phys. Soc. **12**, 316 (1967); R. C. Brandt, thesis, University of Illinois, 1967 (unpublished).
[46] D. C. Burnham, F. C. Brown, and R. S. Knox, Phys. Rev. **119**, 1560 (1960).
[47] F. C. Brown, *Polarons and Excitons*, edited by C. G. Kuper and G. D. Whitfield (Oliver and Boyd, London, 1963), p. 323.
[48] E. J. Johnson and D. M. Larsen, Phys. Rev. Letters **16**, 655 (1966).
[49] D. H. Dickey and D. M. Larsen, Phys. Rev. Letters **20**, 65 (1968).

a strong interaction of the electron with both LO and TO phonons. In AgBr, no peak that may be assigned to the formation of an exciton whose center of mass has an energy equal to that of a TO phonon is observed; the peak assigned to an $n=2$ state of the exciton has an energy that is about 1 meV too high to be assigned to the TO phonon whose energy at low temperature has been accurately measured by Brandt.[45]

Other singularities in the density of states may be assigned to states within the polaron well; these are singularities of the density of states of the "dressed" particle which arise due to the electron-phonon interaction. In an indirect transition the "time during which the transition takes place" is of the order of the inverse of the period of the 8-meV phonon involved. Since it is possible that a polarization well is formed during the optical transition as a result of fluctuations of the polarization field, there may be bound states in this well. It is not clear, however, if the polarization well prepared in this fashion must correspond to a polaron ground state.

The problem has some similarities with the case treated above for the singularity in the density of states $\hbar\omega_0$ above the ground exciton state. When the exciton center of mass has a kinetic energy $\alpha\hbar\omega_0$ there is a state degenerate with it in which a carrier is excited within its polaron well and the center of mass of the exciton is at rest. The quantity α is the electron-lattice (or hole-lattice) coupling constant. In an indirect transition, all final states represented by the exciton and the absorbed (or emitted) phonons have total crystal momentum equal to zero. Since the acoustical phonons involved correspond to a maximum of the phonon branch their momentum may change appreciably without a correspondingly large change of energy. The phonons involved in the transition are therefore a "reservoir of momentum" that guarantees momentum conservation in the interaction between the two polaron states. This feature of the indirect transition, as well as the long times involved, may be necessary conditions for the observation of internal polaron states.

In the case of electron polarons, the electron-lattice coupling constant is known[4,6,47] to be in the neighborhood of 1.7. The ground state of the polaron in its well (self-energy) may be calculated using Feynman's results[50,51]

$$E_p=\hbar\omega_0(\alpha+\beta\alpha^2)$$

for $\alpha\cong 1.7$, $\beta\cong 1.7\times 10^{-2}$.

As far as the author is aware there are no calculations indicating the values of excited polaron states except in the strong coupling limit when the carrier may be excited to the edge of its ground-state polarization well.[52] In the weak coupling limit the polarization energy goes asymptotically to zero[53] as r^{-1}, and an infinite number of highly excited states are expected at the edge of the polarization well.[54] Since excited states at the edge of the polaron well are expected both in the strong and weak coupling limit, it is reasonable to expect them in the range of intermediate couplings ($\alpha\sim 2$). It has to be stressed, however, that these states are not equilibrium states and are not necessarily attainable by the absorption of electromagnetic radiation by a free polaron. They might be attainable by thermal excitation.[52] In these measurements they are observed through the abrupt changes in the density of states they produce.

Experimentally, e.g., in Figs. 4–6, states are observed $E_p=30.1\pm 0.5$ meV both above the singlet and the triplet $1s$ exciton state (2.732 and 2.736 eV); E_p obtained in this fashion is in excellent agreement with what one would expect for the formation of an exciton in either the $1s$ singlet or triplet state in which the electron-polaron is excited to the edge of its well. The coupling constant $\alpha_e=1.68$ is in excellent agreement with Refs. 4 and 6. Notice furthermore that the valley-orbit splitting is unchanged within experimental error indicating that the exciton reduced mass is not changed. This is puzzling if the well is in any way changed from that characteristic of a polaron in its ground state since the well may be pictured as a heavy particle to which the electron is attached by an harmonic force.[50,55] As is expected, these states give rise to rather broad lines. It is difficult to correlate the magnitude of these signals with those of the peaks assigned to the regular excitons since the line shapes are not necessarily the same in both cases, and even if they would be, the linewidths are expected to be different. Confirming this identification, more structure is found $\sim$30 meV above the $n=\infty$ exciton states (2.738 eV). It corresponds to $n=\infty$ excitons in which the electron polaron is excited to the edge of its polarization well (Figs. 4–7).

Only polaron states related to the well characteristic of the polaron in the ground state have been identified. It remains an open question whether polarization wells that are in equilibrium with the carrier in an excited polaron state exist.

The present measurements have determined that 16.4 meV is the ionization energy of an exciton. Brandt[45] determined that the binding energy of a trap (possibly the same that severely limits the electron lifetime at helium temperature[4,47] and gives rise to an electrical glow peak at $\sim$16°K) is 23.8 meV. The energy measured by Brandt is in agreement with what Buimistrov[32] cal-

[50] T. D. Schultz, thesis, Massachusetts Institute of Technology, 1956 (unpublished).

[51] R. P. Feynman, R. W. Hellwarth, C. K. Iddings, and P. M. Platzman, Phys. Rev. **127**, 1004 (1962). See also P. M. Platzman, in *Polarons and Excitons*, edited by C. G. Kuper and G. D. Whitfield (Oliver and Boyd, London, 1963).

[52] S. I. Pekar, *Untersuchen uber die Elektronentheorie der Kristalle* (Akademie-Verlag, Berlin, 1954).

[53] H. Frölich in *Polarons and Excitons*, edited by C. G. Kuper and G. D. Whitefield (Oliver and Boyd, London, 1963), p. 1.

[54] D. Bohm, *Quantum Theory* (Prentice-Hall, Inc., Englewood Cliffs, N. J., 1951), p. 341.

[55] T. D. Schultz, in *Polarons and Excitons*, edited by C. G. Kuper and G. D. Whitefield (Oliver and Boyd, London, 1963), p. 71.

culated for the binding energy of the F center in AgBr (correcting for the low-temperature dielectric constant[56]). The reasonable assumption is made that this energy corresponds to an electron bound to either a vacancy or to some impurity in a fashion reminiscent of a donor atom in the case of Ge and Si. The extremely long lifetimes as well as the complicated kinetics of the decay of the induced optical absorption observed by Brandt appear to give some support to this interpretation.

Buimistrov[32] in his calculation used as unit of energy the rydberg, appropriately reduced by the static dielectric constant of the medium and the reduced *bare mass* of the center. The reduced bare mass of the exciton can therefore be obtained by a comparison of the binding energy that was assigned to the exciton and that of the center studied by Brandt.[45] The resulting ratio of the bare electron and hole masses is $m_e/m_h=0.46$. As in the case of donors in Ge[25] it is likely that the hole mass evaluated in this fashion is close to the lightest mass appearing in the hole effective-mass tensor. The expected corresponding hole-lattice coupling constant is $\alpha_h=2.5$ and the hole polaron binding energy should be 45 meV. The latter two quantities have unknown errors beyond those of the bare hole mass since it is not known whether the same "average" hole mass appears in the expressions for the exciton reduced mass, the hole polaron binding energy, and the coupling constant of the hole polaron.

Experimentally, as may be observed in Figs. 4–7, some broad structure labeled $n=1+\hbar\omega_{\mathrm{LA}}+(\mathrm{pol})_h$ is discernible 52 ± 5 meV above the triplet $1s$ exciton state. It may be assigned to an exciton in which the hole is excited to the edge of its well. From this result one obtains $\alpha_h=3\pm0.3$. Structure observed in Fig. 4(a) (and in other tracings not shown here corresponding to stress in different directions but with smaller resolution than is shown here) at about 2.770 eV [57] is assigned to the case when both the electron and the hole are excited to the edge of their well.

Some of the polaron states described above are still visible in the data taken at 77°K.

VI. CONCLUDING REMARKS

A piezo-optical study has been reported through which the position of the highest maxima of the valence band of AgBr were determined to be along ⟨111⟩. It was shown that the $1s$ exciton state is split by valley-orbit interaction into an orbital triplet and an orbital singlet state 3.8 meV apart. The binding energy of the indirect exciton was measured as equal to 16.4 meV for which, by comparison with the binding energy of an electron in a shallow trap,[32,45] the coupling constant and effective mass of the hole have been evaluated.

The question might be raised whether some of the peaks observed beyond the exciton series limit and assigned to polaron states should instead be assigned to excitons obtained from the split off valence band at L. Contrary to what is observed, it should be expected that this band would give rise to a new series of exciton states, with a different reduced mass; the corresponding piezo-optic peaks should, however, have an amplitude comparable to those observed for the lowest excitons. Photoconductivity data should provide evidence collaborating such an assignment.

Only one large change in photoconductivity that might be assigned to the singularity in the density of states due to the band split by spin-orbit interaction is seen in the data reported in Ref. 1. Following Ref. 7 this peak (2.86 eV) is tentatively assigned to the spin-orbit-split band at L. If this assignment is correct, the spin-orbit splitting at L would be $\sim$165 meV. Although Scop[8] evaluates an upper limit of this splitting as equal to 100 meV it "depends on the difference of two almost identical numbers either of which may be in error by 10%." A spin-orbit splitting of $\sim$165 meV is therefore probably compatible with his calculations.

A final argument can be made against assigning any of the detected states to the spin-orbit-split band at L. It is based on the excellent agreement between the energy of the LO phonon and the electron-polaron–lattice coupling α_e obtained in these experiments and that obtained by other authors from electrical conductivity[4,6,47] and optical measurements.[45] The fact that the exciton series appears to be repeated but shifted by the self-energy of the polaron gives further support to this interpretation.

A series of states characteristic of the polaron have been observed: Exciton states in which the center of mass has a kinetic energy equal to the LO phonon give rise to a singularity in the density of states. Exciton states in which one of the constituting polarons is excited to the edge of its polarization well give rise to other sets of singularities: one when the excited carrier is the electron, another when it is the hole, and finally a third one when both the electron and the hole are excited in their respective polarization wells. The polaron well that is necessary to describe all these states is the well corresponding to a carrier in the ground polaron state.

Some singularities in the densities of states that were expected have not been clearly observed. Although the indirect transition in which the intervening phonon is either LA or TA should be allowed, only one, assigned to LA phonons, is unambiguously observed. The same pattern appears to exist[58] in AgCl. It is hoped that new measurements with better signal-to-noise ratio might lead to the identification of the peak related to the TA phonon.

[56] The author is grateful to Professor H. Kanzaki for pointing out this correction to him.

[57] There is an error in Ref. 19, p. 46, second column, where the comments corresponding to structure at 2.772 and 2.818 eV are obviously interchanged.

[58] G. Ascarelli, Phys. Letters **26A**, 269 (1968).

TABLE II. Summary of the data presented in this paper and comparison with those obtained either by other authors or as a result of calculations.

	This experiment	Other data
LA phonon	7.5 ±0.5 meV	8.05 meV[a]
Exciton B.E.	16.4 ±0.5 meV	23.8 meV (μ/m_e)[b]
Singlet triplet separation	3.5 ±0.5 meV	
Binding energy of the $n=2$ state, of the exciton (2S?)	6.4 ±1 meV	3.8 (μ/m_e) meV[b]
LO phonon	17.4 ±0.5 meV	17.6±0.5 meV[c]
m_h/m_e	2.18±0.2	
m_h^*/m_e^*	2.6 ±0.25	
α_e	1.68±0.01	1.67±0.03[d] 1.69±0.03[e]
α_h	3.0 ±0.3	2.5 (from exciton B.E.)
Binding energy of the electron polaron	30.1 ±0.5 meV	30 ±1 meV[f] 30.2±1 meV[e]
Binding energy of the hole polaron state	52 ±5 meV	45 meV (calc. from exciton B.E.)

[a] Reference 1. [b] Reference 32. [c] Reference 45. [d] References 4 and 47. [e] Reference 6. [f] Reference 4.

Dickey[48] and collaborators reported the observation of the interaction of weakly coupled polarons in InSb with the TO phonons. Singularities of the density of states that might be assigned to this effect have not been observed in AgBr. Such an absence may be expected since the coupling of the polaron with the TO phonon should be much weaker than with the LO phonon at $k=0$ on account of the polarization field associated with the latter.

The question may be asked whether states exist in which the polarization well associated with a carrier corresponds to an excited rather than a ground polaron state. Such states are not unambiguously observed. The polaron mass should be smaller than the mass contributing to the regular exciton and therefore the binding energy of the exciton might be decreased. The principal results of this study are summarized in Table II.

ACKNOWLEDGMENTS

The author is grateful to many of his colleagues, in particular to Professor P. Fisher, Professor A. K. Ramdas, Professor E. W. Prohofsky, Professor L. Van-Zandt and Dr. Y. Yafet for many helpful discussions. He is particularly grateful to Professors E. W. Prohofsky, Professor A. K. Ramdas and Professor S. Rodriguez for critically reading the manuscript. He thanks Dr. R. Van Heyningen and Dr. F. Moser of the Kodak Research Laboratories, and Dr. James E. Luvalle of the Fairchild Space and Defense System for providing, respectively, the AgBr precipitate and the zone-refined ingot that made this study possible. He wishes to thank Professor D. W. Lynch and Professor F. C. Brown for the communication of their results prior to publication.

APPENDIX A: SYMMETRY OF EXCITON, BAND, AND PHONON STATES

Many of the arguments in this paper were based on the characterization of the phonons, electronic energy bands, and indirect excitons in terms of the representations of the cubic group. These representations will be obtained in this appendix.

On account of the degeneracy of the different valence-band maxima it is not possible to assign an electron to a given valence-band maximum but rather this electron is shared by many of the equivalent maxima. Linear combinations of the wave functions describing electrons in the different valence-band maxima will form a basis of the representations of the cubic group $\bar{O}_h$. These representations are generated from those corresponding to a single $\langle 111\rangle$ valence-band maximum by the application of Frobenius's reciprocity theorem.[27,59]

Table III is the compatibility[28] table for $\bar{O}_h$. It can be seen that the single group representation Γ_3^- (L_3^- in the notation of Ref. 7) of D_{3d} that describes the top of the valence band at L[7,8] is contained in Γ_3^-, Γ_4^-, and Γ_5^- of O_h. According to Frobenius's theorem the required linear combinations of valence-band wave functions at L that form a basis of the Γ_3^- representation of D_{3d} will transform like $(\Gamma_3^-+\Gamma_4^-+\Gamma_5^-)$ of O_h. In the perfect crystal, these representations correspond to states that have the same energy—they will only be split by an external perturbation.

When spin-orbit coupling is taken into account, the states at the top of the valence band form a basis of the Γ_5^- and Γ_6^- representations of $\bar{D}_{3d}$ (L_4^- and L_5^- in the notation of Ref. 7). The energies corresponding to these two one-dimensional representations are degenerate in the absence of a magnetic field due to time reversal.[60] From Table III it is seen that the one-dimensional representation Γ_5^- of $\bar{D}_{3d}$ is contained in the four-dimensional representation Γ_8^- of $\bar{O}_h$. Also Γ_6^- of $\bar{D}_{3d}$ is contained in Γ_8^- of $\bar{O}_h$. The linear combinations of the wave functions corresponding to the maxima of the valence band at L form, therefore, two degenerate sets of linear combinations that transform like Γ_8^- of $\bar{O}_h$.

The representation of Wannier excitons that corresponds to a conduction and a valence band that are at the center of the Bz is equal to the product of the representations of the valence band, the conduction band, and the envelope wave function obtained from an effective-mass equation.[30] In the case of an indirect exciton the representation of the valence band, conduction band, and the envelope function that appear in the product must belong to the same group, in this case $\bar{O}_h$. The ground state of the exciton should have a $1s$-like envelope wave function that transforms like Γ_1^+ when the symmetry is decreased from the spherical to the cubic case. A p-like envelope would correspond to a Γ_4^- representation, etc.

The wave function of the $1s$ indirect exciton obtained from holes whose symmetry is Γ_5^- or Γ_6^- and electrons whose symmetry is Γ_6^+ is

$$\Gamma_1^+\times 2\Gamma_8^-\times\Gamma_6^+=2\Gamma_3^-+2\Gamma_4^-+2\Gamma_5^-. \quad \text{(A1)}$$

[59] F. D. Murnaghan, *The Theory of Group Representation* (The Johns Hopkins Press, Baltimore, 1938), p. 100.
[60] V. Heine, *Group Theory in Quantum Mechanics* (Pergamon Press, Oxford, 1964), p. 164.

TABLE III. Compatibility table of the group O_h. The reduction of symmetry from the cubic group to D_{2h} may be accomplished in two different ways: either the crystal is compressed by different amounts along two ⟨100⟩ directions or it is compressed along ⟨110⟩. The system of orthogonal axes of these two groups are not the same; the compatibility tables relating the two possible D_{2h} groups to the D_{4h} group are therefore different. Table 41 of Koster *et al.*[a] refers to the former case. The data corresponding to D_{2h} in this table is obtained from E. B. Wilson, Jr., *et al.*[b]

$\bar{O}_h$	$\Gamma_1^{\pm}$	$\Gamma_2^{\pm}$	$\Gamma_3^{\pm}$	$\Gamma_4^{\pm}$	$\Gamma_5^{\pm}$	$\Gamma_6^{\pm}$	$\Gamma_7^{\pm}$	$\Gamma_8^{\pm}$
$\bar{D}_{4h}$	$\Gamma_1^{\pm}$	$\Gamma_2^{\pm}$	$\Gamma_1^{\pm}+\Gamma_3^{\pm}$	$\Gamma_2^{\pm}+\Gamma_5^{\pm}$	$\Gamma_4^{\pm}+\Gamma_5^{\pm}$	$\Gamma_6^{\pm}$	$\Gamma_7^{\pm}$	$\Gamma_6^{\pm}+\Gamma_7^{\pm}$
$\bar{D}_{2h}$	$\Gamma_1^{\pm}$	$\Gamma_3^{\pm}$	$\Gamma_1^{\pm}+\Gamma_3^{\pm}$	$\Gamma_2^{\pm}+\Gamma_3^{\pm}+\Gamma_4^{\pm}$	$\Gamma_1^{\pm}+\Gamma_2^{\pm}+\Gamma_4^{\pm}$	$\Gamma_5^{\pm}$	$\Gamma_5^{\pm}$	$2\Gamma_5^{\pm}$
$\bar{D}_{3d}$	$\Gamma_1^{\pm}$	$\Gamma_2^{\pm}$	$\Gamma_3^{\pm}$	$\Gamma_2^{\pm}+\Gamma_3^{\pm}$	$\Gamma_1^{\pm}+\Gamma_3^{\pm}$	$\Gamma_4^{\pm}$	$\Gamma_4^{\pm}$	$\Gamma_4^{\pm}+\Gamma_5^{\pm}+\Gamma_6^{\pm}$

[a] Reference 28.
[b] E. B. Wilson, Jr., J. C. Decius, and P. C. Cross, *Molecular Vibrations* (McGraw-Hill Book Co., New York, 1965), p. 336.

Γ_6^+ is the representation of the conduction band at Γ in the double-group notation. The dimensionality of the Γ_3^-, Γ_4^-, and Γ_5^- representations is respectively 2, 3, and 3.

Each "orbital" exciton state is fourfold degenerate in the approximation in which both the magnetic interaction between the electron and the hole and the difference between the longitudinal and transverse excitons is neglected.[30,61] The spin-orbit interaction of the electron and hole with the crystalline potential has been taken into account in the band specification. On the basis of the experimental evidence presented in Sec. III the *s*-like indirect exciton states at L are split into a "singlet" ($2\Gamma_3^-$) and a "triplet" ($2(\Gamma_4^-+\Gamma_5^-)$). An eventual spin splitting, e.g., between the two sets of Γ_3^- states, is not necessarily the same as in the case of positronium[62] (8×10^{-4} eV) since both the hole and electron are not equivalent particles that differ just by the sign of their charge, but each one is instead differently coupled to the remaining carriers in their respective bands. This is reflected in the g factor of both the electron and hole that are not necessarily equal to 2; the g tensor of the holes is indeed expected to be anisotropic. Even if the deviations of the g factors from 2 are negligible, the Fermi contact interaction between the electron and the hole will be decreased from that of positronium by approximately the cube of the ratio of the Bohr radii of positronium and the exciton. This would bring the expected interaction energy into the megacycle region.

The exchange interaction between an electron and a hole on the same atom contributes to the spin-spin splitting.[61] Following Elliot[63] it may be assumed that for this purpose the wave functions corresponding to the valence- and conduction-band extrema are similar to the $4d$ and $5s$ wave functions of Ag^+; the exchange interaction (J_{eff}) can then be estimated from the $^3D-{}^1D$ splitting[64] (J) of the $4d^95s$ states of Ag^+. In view of the above assumption it is likely that the result will overestimate this splitting:

$$J_{\text{eff}}\simeq\tfrac{1}{4}[\Omega|\Phi(0)|^2J],$$

where Ω is the volume of the unit cell of AgBr, $|\Phi(0)|^2=(\pi a^{*3})^{-1}$, $a^*\sim23$ Å is the Bohr radius of the exciton, and $J\simeq2300$ cm^{-1}. The resulting estimate of J_{eff} is 0.3 cm^{-1}.

Both the spin-spin interactions considered above and the interaction giving rise to the longitudinal and transverse excitons[61] may split the triplet state. The former splitting is probably smaller than the spin-spin term originating from the exchange interaction considered previously since for the triplet $|\Phi(0)|^2$ is expected to be smaller than in the case of the singlet state.

An attempt may be made to understand the origin of the exciton states by considering the mixture of p and d tight-binding states that gives rise to the valence-band maximum[7] at L. Since *s*-like exciton states are considered, the envelope wave function transforms like D_0^+ of the full rotation group. The $S_{1/2}$ conduction-band electron wave function transforms like $D_{1/2}^+$ while the valence-band wave functions that are a linear combination of p and d wave functions transform like $D_{1/2}^-+D_{3/2}^-+D_{3/2}^-+D_{5/2}^-$. The total exciton wave function in the atomic spherically symmetric case is therefore (spin-orbit interaction has been neglected)

$$D_0^+\times(D_{1/2}^-+2D_{3/2}^-+D_{5/2}^-)\times D_{1/2}^+=D_{\text{ex}}, \quad \text{(A2)}$$

where

$$D_0^+\times D_{1/2}^-\times D_{1/2}^+=D_0^-+D_1^-,$$

$$2(D_0^+\times D_{3/2}^-\times D_{1/2}^+)=2(D_1^-+D_2^-),$$

and

$$D_0^+\times D_{5/2}^-\times D_{1/2}^+=D_2^-+D_3^-.$$

When the symmetry is reduced from spherical to cubic,

$$D_0^-+D_1^-\rightarrow\Gamma_1^-+\Gamma_4^-, \quad \text{(A3)}$$

$$2(D_1^-+D_2^-)\rightarrow2(\Gamma_3^-+\Gamma_4^-+\Gamma_5^-), \quad \text{(A4)}$$

$$(D_2^-+D_3^-)\rightarrow\Gamma_2^-+\Gamma_3^-+\Gamma_4^-+2\Gamma_5^-. \quad \text{(A5)}$$

The exciton states obtained from the L_4^- and L_5^- valence-band maxima[7] arise therefore from the $J=\frac{3}{2}$-like valence-band states. The remaining representations correspond to exciton states obtained from the split-off valence band at L whose symmetry[7] is L_6^-.

The reduction of crystal symmetry produced by stress will split the exciton lines further.[33] When the applied force is along ⟨111⟩ the symmetry of the crystal is $\bar{D}_{3d}$; the singlet exciton still transforms according to two

[61] R. S. Knox, *Theory of Excitons* (Academic Press Inc., New York, 1963), pp. 24, 45.
[62] S. DeBenedetti and H. C. Corben, Ann. Rev. Nucl. Sci. 4, 191 (1954).
[63] R. J. Elliot, Phys. Rev. 124, 340 (1961).
[64] C. E. Moore, Natl. Bur. Std. (U. S.) Circ. 467, 51 (1958).

representations Γ_3^- while the triplet transforms according to $2(\Gamma_1^-+\Gamma_2^-)+4\Gamma_3^-$. From Ref. 33 the split triplet must correspond to an orbital singlet and an orbital doublet. It is not possible to decide on the basis of group theory how the states corresponding to the different representations associate. The choice between the two different alternatives is determined by the fact that agreement between the predicted and measured relative magnitude of the piezo-optic signal arising from the singlet and triplet states can be obtained only by associating states whose symmetry is $(\Gamma_1^-+\Gamma_2^-+\Gamma_3^-)$ that are split from states whose symmetry is $(\Gamma_1^-+\Gamma_2^-+3\Gamma_3^-)$ (Appendix B). The same arguments determine that the states into which the triplet is split under a $\langle 110\rangle$ stress have symmetries $4\Gamma_4^-$, $2(\Gamma_1^-+\Gamma_3^-)$, and $4\Gamma_2^-$.

Group theory and deformation potential theory[34,38] permit the choice of the different associations of LA phonon symmetries in the stressed crystal.[27]

Under a $\langle 111\rangle$ stress the LA phonons at L split into a group of three states separated from a fourth one.[38] The representations corresponding to the split phonon states are Γ_1^+ and $(\Gamma_1^++\Gamma_3^+)$. This conclusion can be reached either on the basis of the dimensionalities of the representations of the phonon states or on the basis of the fact that in the deformed crystal the group of one of the k vectors at L remains D_{3d} while those of the other three belong to C_{2h}. The wave functions of the LA phonons form a basis for the Γ_1^+ representations of either D_{3d} or C_{2h} (Table III). The wave functions that form a basis of the Γ_1^+ representation of C_{2h} generate, according to Frobenius's theorem,[27,59] wave functions that form a basis of the $(\Gamma_1^++\Gamma_3^+)$ representations of the group of the stressed crystal (D_{3d}).

Under a $\langle 110\rangle$ stress the new crystal symmetry is D_{2h} and the four phonons at L split into two groups of two.[38] The group of the corresponding k vectors are $C_{2h}(x)$ and $C_{2h}(y)$. The phonon whose local symmetry was Γ_1^+ of D_{3d} is either Γ_1^+ of $C_{2h}(x)$ or Γ_1^+ of $C_{2h}(y)$ in the stressed crystal. Using again Frobenius's theorem,[59] it is seen that the Γ_1^+ representation of $C_{2h}(x)$ generates the Γ_1^+ and Γ_4^+ representations of D_{2h} while the Γ_1^+ representation of $C_{2h}(y)$ generates the Γ_1^+ and Γ_2^+ representations of D_{2h}. The four phonon states are therefore split into $(\Gamma^++\Gamma_4^+)$ and $(\Gamma_1^++\Gamma_2^+)$. The same symmetry components may be obtained from Table III by the reduction of the $(\Gamma_1^++\Gamma_5^+)$ representations of O_h.

APPENDIX B: CALCULATION OF THE RELATIVE MAGNITUDES OF THE EXCITON PEAKS

In this appendix the details for the calculation of the relative magnitudes of the singlet and triplet piezo-optic exciton peaks are illustrated.

Consider an external force directed along $\langle 111\rangle$ and assume that the triplet exciton state is split into a group of four states that transform as $(\Gamma_1^-+\Gamma_2^-+\Gamma_3^-)$, whose energy is *increased* above the center of gravity of the exciton states[31] by $(2/9)\Xi_u^v s_{44}\tau$, while the energy of the remaining states $(\Gamma_1^-+\Gamma_2^-+3\Gamma_3^-)$ originating from the triplet exciton decreases[33] by $\frac{1}{9}\Xi_u^v s_{44}\tau$. The energy of the singlet exciton state instead deviates only quadratically from that of the center of gravity of the exciton states. The quadratic energy shift is undetectable in the present experiment; only the term corresponding to the shift of the center of gravity of the exciton, $(\Xi_c+\Xi_d^v+\frac{1}{3}\Xi_u^v)(s_{11}+2s_{12})\tau$, contributes to the piezo-optic signal. The shear and longitudinal deformation potentials of the valence band at L are, respectively, Ξ_u^v and Ξ_d^v; Ξ_c is the deformation potential of the conduction band,[35] and s_{11}, s_{12}, and s_{44} are the compliance constants of the crystal. The LA phonon states are split in a way that is similar to that of the electronic bands at L.[12,34,38] The corresponding deformation potentials are Ξ_d^p and Ξ_u^p. It is assumed that the energy of the Γ_1^+ phonon state is increased with stress respect to the energy of the center of gravity of the phonon states by $(3/9)\Xi_u^p s_{44}\tau$ while the energy of the remaining states, that transform like $(\Gamma_1^++\Gamma_3^+)$ of D_{3d}, is decreased by $\frac{1}{9}\Xi_u^p s_{44}\tau$ with respect to the center of gravity of the phonon states.[38] The center of gravity of the phonon states increases by $(\Xi_d^p+\frac{1}{3}\Xi_u^p)(s_{11}+2s_{12})\tau$ (see Fig. 2).

The optical transition takes place with the absorption of a photon and the absorption (or emission) of a phonon. The results described previously indicate that the most important intermediate state must involve the Γ_8 band. The appropriate indirect exciton states Γ_5 involving the $(L_4^-+L_5^-)$ valence band and the Γ_8^+ conduction band for which the product $\Gamma_s\Gamma_4^-\Gamma_{ex}$ contains Γ_1^+ are p-like exciton states. Their symmetry is $\Gamma_s=\Gamma_8^-\Gamma_8^+\Gamma_4^-=2(\Gamma_1^++\Gamma_2^++2\Gamma_3^++3\Gamma_4^++3\Gamma_5^+)$.

Only intermediate states whose wave functions form a basis of Γ_1^+ and Γ_5^+ can be attained from a Γ_1^+ initial state by the absorption of a LA phonon whose symmetry is $(\Gamma_1^++\Gamma_5^+)$. The remaining exciton states having Γ_2^+, Γ_3^+, and Γ_4^+ symmetry are important intermediate states for the indirect absorption in which a TA phonon is involved.

In the following calculation it will be assumed that the above p-like excitons are the principal contributors to the sum over intermediate states that appear in the absorption coefficient. The justifications for this assumptions are the experimental results quoted previously (Sec. III).

Piezo-Optic Signal due to Exciton States

The splitting produced by a $\langle 111\rangle$ force on the different phonon and exciton states whose changes in energy appear in $dE_{cr}/d\tau$ are shown in Fig. 2. Only the intermediate states whose symmetry is such that they are attainable with a LA phonon (that form a basis for the Γ_1^+ and Γ_3^+ representations) have been sketched in the figure. Of these there are eight two-dimensional Γ_3^+ representations and four one-dimensional Γ_1^+ representations. In the stressed crystal, the electric dipole opera-

tor has Γ_2^- symmetry for light polarized parallel to the applied force and Γ_3^- symmetry for light polarized perpendicular to the applied force. The quantity $\Gamma_s\Gamma_3^-\Gamma_{ex}$ in which $\Gamma_s=\Gamma_1^+$ contains Γ_1^+ only if $\Gamma_{ex}=\Gamma_3^-$. If $\Gamma_s=\Gamma_3^+$ the above product contains Γ_1^+ only if $\Gamma_{ex}=\Gamma_1^-$, Γ_2^-, or Γ_3^-.

Consider, therefore, the contribution to $dE_{cr}/d\tau$ arising from the state whose symmetry is Γ_3^- that originates from the triplet exciton by an energy shift of $(2/9)\Xi_u{}^v s_{44}\tau$ with respect to the exciton center of gravity. Consider, furthermore, transitions having an intermediate exciton state whose symmetry is Γ_1^+.

The final Γ_3^- exciton state is doubly degenerate. There are four Γ_1^+ intermediate states that may be reached with two distinct Γ_1^+ phonons. Each one of the states forming the Γ_3^- state can therefore be reached in 4×2 ways. There are therefore 8×2 equal terms in the sum appearing in Eq. (10) that correspond to the same final state. The contribution to $dE_{cr}/d\tau$ from this state is, therefore,

$$16[(\Xi_c+\Xi_d{}^v+\tfrac{1}{3}\Xi_u{}^v)(s_{11}+2s_{12})+(2/9)\Xi_u{}^v s_{44} \pm(\Xi_d{}^p+\tfrac{1}{3}\Xi_u{}^p)(s_{11}+2s_{12})\pm(3/9-\tfrac{1}{9})\Xi_u{}^p s_{44}].$$

The first two terms describe the energy shift of the Γ_3^- state while the remaining two terms describe the energy shift of the Γ_1^+ phonons. The plus sign refers to the case when a phonon is emitted while the minus sign refers to the case when the phonon is absorbed.

Although tedious, it is simple to take into account all terms that arise from both the singlet and the triplet exciton state. Calling

$$(P_\perp)_t{}^{\langle111\rangle}=(dE_{cr}/d\tau)(\delta^t)^{-1/2}|\Phi_t(0)|^2 d\tau$$

the piezo-optic signal obtained from the triplet state observed with light polarized perpendicular to the $\langle111\rangle$ stress, and using corresponding notations for the singlet and for the case of parallel ($\|$) polarization, one obtains (case of the emitted phonon)

$$\left\{\frac{(P_\perp)_t}{(P_\perp)_s}\right\}^{\langle111\rangle}=\frac{28-\frac{1}{3}x-(4/3)y}{8-8(y/9)}\varphi, \quad \text{(B1)}$$

$$\left\{\frac{(P_\|)_t}{(P_\|)_s}\right\}^{\langle111\rangle}=\frac{26+\frac{1}{3}x-(20/9)y}{8-8(y/9)}\varphi, \quad \text{(B2)}$$

$$\{(P_\perp)_t/(P_\perp)_s\}^{\langle110\rangle}=(3-\tfrac{1}{3}x)\varphi, \quad \text{(B3)}$$

$$\{(P_\|)_t/(P_\|)_s\}^{\langle110\rangle}=(3+\tfrac{1}{3}x)\varphi. \quad \text{(B4)}$$

The quantities x, y, and φ are defined below for the case when a phonon is emitted:

$$x=\frac{\Xi_u{}^v s_{44}}{[\Xi_c+\Xi_d{}^v+\Xi_d{}^p+\frac{1}{3}(\Xi_u{}^v+\Xi_u{}^p)](s_{11}+2s_{12})}, \quad \text{(B5)}$$

$$y=\frac{\Xi_u{}^p s_{44}}{[\Xi_c+\Xi_d{}^v+\Xi_d{}^p+\frac{1}{3}(\Xi_u{}^v+\Xi_u{}^p)](s_{11}+2s_{12})}, \quad \text{(B6)}$$

$$\varphi=|\Phi_t(0)|^2(\delta^s)^{1/2}/|\Phi_s(0)|^2(\delta^t)^{1/2}. \quad \text{(B7)}$$

Remembering that a $\langle100\rangle$ stress does not remove the degeneracy of either the final exciton states or the phonon degeneracy,[34,38] the ratio of the expected piezo-optic signals are in this case just φ times the ratios of the number of terms appearing in Eq. (10). Therefore, from Fig. 2 (unstressed crystal)

$$\left\{\frac{(P_\perp)_t}{(P_\perp)_s}\right\}^{\langle100\rangle}=\left\{\frac{(P_\|)_t}{(P_\|)_s}\right\}^{\langle100\rangle}=\frac{165}{54}\varphi=7.8. \quad \text{(B8)}$$

The observed values of the different ratios of peak heights for the triplet and singlet exciton are (the way in which the background has been taken into account is shown in the broken lines of Figs. 4–6)

$$\begin{aligned}&\{(P_\perp)_t/(P_\perp)_s\}^{\langle110\rangle}=15, \quad \{(P_\|)_t/(P_\|)_s\}^{\langle110\rangle}=1/6.5,\\ &\{(P_\|)_t/(P_\|)_s\}^{\langle111\rangle}=-\tfrac{3}{4}, \quad \{(P_\perp)_t/(P_\perp)_s\}^{\langle111\rangle}=25, \quad \text{(B9)}\\ &\{(P_\perp)_t/(P_\perp)_s\}^{\langle100\rangle}=7.2, \quad \{(P_\|)_t/(P_\|)_s\}^{\langle100\rangle}=6.3.\end{aligned}$$

Using the first three values above, one obtains $x=-8.7$, $\varphi=2.54$, $y=1.1$, from which one predicts

$$\{(P_\perp)_t/(P_\perp)_s\}^{\langle111\rangle}=20.7.$$

This has to be compared with the magnitude of 25 that is observed. Considering the errors involved in the evaluation of the relative magnitudes of the different peaks the agreement is excellent.

Under the assumption that the triplet state is split by a $\langle111\rangle$ force into two groups of states whose symmetry is, respectively, $4\Gamma_3^-$ and $2(\Gamma_1^-+\Gamma_2^-)$, the predicted ratio $\{(P_\perp)_t/(P_\perp)_s\}^{\langle111\rangle}$ is instead ~2. A different splitting in the case of a $\langle110\rangle$ stress results in

$$\{(P_\perp)_t/(P_\perp)_s\}^{\langle110\rangle}=\{(P_\|)_t/(P_\|)_s\}^{\langle110\rangle}.$$

Upon using these same ratios of deformation potentials to fit the peaks that correspond to the case when a phonon is absorbed rather than emitted it is determined that the quantities $(\Xi_c+\Xi_d{}^v+\frac{1}{3}\Xi_u{}^v)$ and $(\Xi_d{}^p+\frac{1}{3}\Xi_u{}^p)$ are almost equal. The same conclusion is reached on the basis of preliminary measurements involving both a large static and a small dynamic stress. From hydrostatic pressure measurements, Brothers and Lynch[65] conclude that $3[\Xi_c+\Xi_d{}^v+\Xi_d{}^p+\frac{1}{3}(\Xi_u{}^v+\Xi_u{}^p)](s_{11}+2s_{12})=-1.9\times10^{-6}$ eV/atm. From these data, in conjunction with the results of the analysis of the magnitude of the piezo-optic signal assigned to the singlet and triplet exciton, both the magnitudes of $\Xi_u{}^v s_{44}$ and $\Xi_u{}^p s_{44}$ can be evaluated as, respectively, equal to 5.5×10^{-6} and -0.7×10^{-6} eV/atm. The quantities $\Xi_u{}^v$ and $\Xi_u{}^p$ are therefore ~4.3 and -0.58 eV. The accuracy of the relative values of the deformation potentials is expected to be about 40%.

Note added in the proof. Another suitable intermediate state would be a direct s-like exciton at Γ formed by an electron in a Γ_6^+ conduction band and a hole in a Γ_8^- valence band. This state would be reached by means of

[65] A. D. Brothers and D. W. Lynch (private communication).

the absorption of a photon. The only states of the exciton multiplet ($\Gamma_3^-+\Gamma_4^-+\Gamma_5^-$) that are important are therefore the Γ_4^- states. The transition to the final exciton states could take place by means of a ($\Gamma_1^++\Gamma_5^+$) phonon. Assuming the same ordering of stressed states as in the text one obtains

$$\left\{\frac{(P_\perp)_t}{(P_\perp)_s}\right\}^{\langle 111\rangle}=\frac{10-\frac{1}{9}x-2y/9}{4}\varphi, \tag{B10}$$

$$\left\{\frac{(P_{11})_t}{(P_{11})_s}\right\}^{\langle 111\rangle}=\frac{10-\frac{1}{9}x-\frac{2}{3}y}{4-4y/9}\varphi, \tag{B11}$$

$$\{(P_\perp)_t/(P_\perp)_s\}^{\langle 110\rangle}=(3-\tfrac{1}{6}x)\varphi, \tag{B12}$$

$$\{(P_{11})_t/(P_{11})_s\}^{\langle 110\rangle}=(3+\tfrac{1}{6}x)\varphi, \tag{B13}$$

$$\{(P_{11})_t/(P_{11})_s\}^{\langle 100\rangle}=\{(P_\perp)_t/(P_\perp)_s\}^{\langle 100\rangle}=\{(P)_t/(P)_s\}_{\substack{\text{wavelength}\\ \text{modulation}}}=(21/6)\varphi. \tag{B14}$$

Taking the experimental values given in (B9) one obtains $\varphi=2.57$, $x=-17.7$, $y=16.3$ and calculates

$$\left\{\frac{(P_\perp)_t}{(P_\perp)_s}\right\}^{\langle 111\rangle}=5.29.$$

The calculated ratio of the same peaks observed with wavelength modulation or ⟨100⟩ stress is equal to 9. The observed wavelength modulation value[66] is 7.8±0.5. If the alternate association of exciton states discussed at the end of Appendix A is chosen for the case of a ⟨110⟩ stress one obtains $\varphi=5$ and the expected ratio of the wavelength modulation signals would be 17.5. If the alternate choice of exciton states split by ⟨111⟩ stress is taken, the predicted value of $\{(P_\perp)_t/(P_\perp)_s\}^{\langle 111\rangle}$ is 8.5. The parameter $\varphi=2.57$.

APPENDIX C: MEASUREMENTS OF ELASTIC CONSTANTS

Extensive measurements of elastic constants were made by Tannhauser *et al.*[67] above room temperature. Expansion-coefficient measurements were made by Strelkow[68] in the same range.

The frequency f of the extensional mechanical resonance of the samples is

$$f=(2l)^{-1}(Y/\rho)^{1/2}, \tag{C1}$$

where l is the length of the sample, ρ is its density, and Y is its Young modulus given by[69]

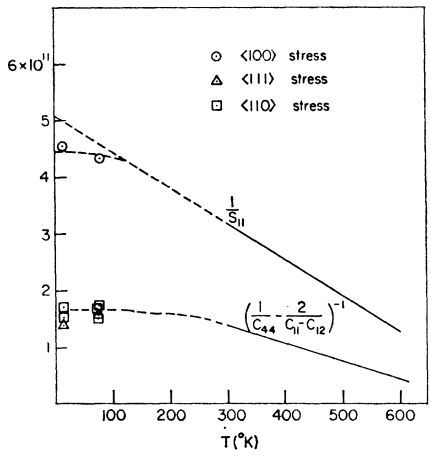

FIG. 15. Temperature dependence of the combinations of elastic constants that can be obtained from the measurement of Young's modulus. The solid line is calculated using the data of Ref. 64.

$$\frac{1}{Y}=\frac{(c_{11}+c_{12})}{(c_{11}+2c_{12})(c_{11}-c_{12})}+\left(\frac{1}{c_{44}}-\frac{2}{c_{11}-c_{12}}\right)\times(n_x^2n_y^2+n_x^2n_z^2+n_y^2n_z^2) \tag{C2}$$

or

$$\frac{1}{Y}=s_{11}+[s_{44}-2(s_{11}-s_{12})]\times(n_x^2n_y^2+n_y^2n_z^2+n_x^2n_z^2). \tag{C3}$$

The quantities c_{ij} are the elastic constants, the s_{ij} are the complicance coefficients, and n_x, n_y, n_z are the direction cosines with respect to the cubic axes of a vector parallel to the length of the sample.

The value of the quantities s_{11} and $(1/c_{44}-2/(c_{11}-c_{12}))^{-1}$ at different temperatures are obtained by comparing the ratio of Young's modulus at temperature T and at room temperature for samples whose length is along ⟨111⟩, ⟨100⟩, and ⟨110⟩. A correction for thermal expansion has to be considered. The expansion coefficient is obtained by a linear extrapolation towards low temperatures of Strelkov's[67] data. The room-temperature elastic constants above room temperature are given in Ref. 66. The results of the present measurements are given in Fig. 15.

The accuracy of the result is probably of the order of ±5% since the electrodes developed on the sample affect the measurements. This is the major source of scatter of the measured data since the resonant frequency depends to some extent on the thickness of the developed electrodes and to a smaller extent on the amplitude of the exciting force. Both at room temperature and at liquid-nitrogen temperature, when the amplitude of vibration of the strain was of the order of 10^{-6}, changes in elastic constants of a few parts per thousand were noticed.

[66] G. Ascarelli (to be published).
[67] D. S. Tannhauser, L. J. Bruner, and A. W. Lawson, Phys. Rev. **102**, 1276 (1956).
[68] P. G. Strelkov, Physik Z. Sowjetunion **12**, 77 (1937).
[69] L. D. Landau and E. M. Lifshitz, *Theory of Elasticity* (Pergamon Press, Inc., London, 1959), p. 42.